

Numerical Investigations of Virus Transport Aboard a Commuter Bus

Hamid Rahai, PhD

Jeremy Bonifacio, PhD



MINETA TRANSPORTATION INSTITUTE

Founded in 1991, the Mineta Transportation Institute (MTI), an organized research and training unit in partnership with the Lucas College and Graduate School of Business at San José State University (SJSU), increases mobility for all by improving the safety, efficiency, accessibility, and convenience of our nation's transportation system. Through research, education, workforce development, and technology transfer, we help create a connected world. MTI leads the [Mineta Consortium for Transportation Mobility \(MCTM\)](#) funded by the U.S. Department of Transportation and the [California State University Transportation Consortium \(CSUTC\)](#) funded by the State of California through Senate Bill 1. MTI focuses on three primary responsibilities:

Research

MTI conducts multi-disciplinary research focused on surface transportation that contributes to effective decision making. Research areas include: active transportation; planning and policy; security and counterterrorism; sustainable transportation and land use; transit and passenger rail; transportation engineering; transportation finance; transportation technology; and workforce and labor. MTI research publications undergo expert peer review to ensure the quality of the research.

Education and Workforce Development

To ensure the efficient movement of people and products, we must prepare a new cohort of transportation professionals who are ready to lead a more diverse, inclusive, and equitable transportation industry. To help achieve this, MTI sponsors a suite of workforce development and education opportunities. The Institute supports educational programs offered by the Lucas Graduate School of Business: a Master of Science in Transportation Management, plus graduate certificates that include High-Speed and Intercity Rail Management and Transportation Security Management. These flexible programs offer live online classes so that working transportation professionals can pursue an advanced degree regardless of their location.

Information and Technology Transfer

MTI utilizes a diverse array of dissemination methods and media to ensure research results reach those responsible for managing change. These methods include publication, seminars, workshops, websites, social media, webinars, and other technology transfer mechanisms. Additionally, MTI promotes the availability of completed research to professional organizations and works to integrate the research findings into the graduate education program. MTI's extensive collection of transportation-related publications is integrated into San José State University's world-class Martin Luther King, Jr. Library.

Disclaimer

The contents of this report reflect the views of the authors, who are responsible for the facts and accuracy of the information presented herein. This document is disseminated in the interest of information exchange. MTI's research is funded, partially or entirely, by grants from the U.S. Department of Transportation, the U.S. Department of Homeland Security, the California Department of Transportation, and the California State University Office of the Chancellor, who assume no liability for the contents or use thereof. This report does not constitute a standard specification, design standard, or regulation.

Report 21-07

Numerical Investigations of Virus Transport Aboard a Commuter Bus

Hamid Rahai, PhD
Jeremy Bonifacio, PhD

April 2021

A publication of the
Mineta Transportation Institute
Created by Congress in 1991

College of Business
San José State University
San José, CA 951920219

TECHNICAL REPORT DOCUMENTATION PAGE

| | | | |
|---|---|--|------------------|
| 1. Report No. 21-07 | 2. Government Accession No. | 3. Recipient's Catalog No. | |
| 4. Title and Subtitle Numerical Investigations of Virus Transport Aboard a Commuter Bus | | 5. Report Date April 2021 | |
| | | 6. Performing Organization Code | |
| 7. Authors Hamid Rahai, PhD Jeremy Bonifacio, PhD | | 8. Performing Organization Report CA-MTI-2048 | |
| 9. Performing Organization Name and Address Mineta Transportation Institute College of Business, San José State University San José, CA 95192-0219 | | 10. Work Unit No. | |
| | | 11. Contract or Grant No. ZSB12017-SJAUX | |
| 12. Sponsoring Agency Name and Address State of California SB1 2017/2018 Trustees of the California State University Sponsored Programs Administration 401 Golden Shore, 5th Floor Long Beach, CA 90802 | | 13. Type of Report and Period Covered Final Report | |
| | | 14. Sponsoring Agency Code | |
| 15. Supplemental Notes DOI: 10.31979/mti.2021.2048 | | | |
| 16. Abstract <p>The authors performed unsteady numerical simulations of virus/particle transport released from a hypothetical passenger aboard a commuter bus. The bus model was sized according to a typical city bus used to transport passengers within the city of Long Beach in California. The simulations were performed for the bus in transit and when the bus was at a bus stop opening the middle doors for 30 seconds for passenger boarding and drop off. The infected passenger was sitting in an aisle seat in the middle of the bus, releasing 1267 particles (viruses)/min. The bus ventilation system released air from two linear slots in the ceiling at 2097 cubic feet per minute (CFM) and the air was exhausted at the back of the bus. Results indicated high exposure for passengers sitting behind the infectious during the bus transit. With air exchange outside during the bus stop, particles were spread to seats in front of the infectious passenger, thus increasing the risk of infection for the passengers sitting in front of the infectious person. With higher exposure time, the risk of infection is increased.</p> <p>One of the most important factors in assessing infection risk of respiratory diseases is the spatial distribution of the airborne pathogens. The deposition of the particles/viruses within the human respiratory system depends on the size, shape, and weight of the virus, the morphology of the respiratory tract, as well as the subject's breathing pattern. For the current investigation, the viruses are modeled as solid particles of fixed size. While the results provide details of particles transport within a bus along with the probable risk of infection for a short duration, however, these results should be taken as preliminary as there are other significant factors such as the virus's survival rate, the size distribution of the virus, and the space ventilation rate and mixing that contribute to the risk of infection and have not been taken into account in this investigation.</p> | | | |
| 17. Key Words Virus dispersion, Particle transport, Mixing and diffusion, Turbulence, Environmental health | | 18. Distribution Statement No restrictions. This document is available to the public through The National Technical Information Service, Springfield, VA 22161 | |
| 19. Security Classif. (of this report) Unclassified | 20. Security Classif. (of this page) Unclassified | 21. No. of Pages 32 | 22. Price |

Copyright © 2021

by **Mineta Transportation Institute**

All rights reserved.

DOI: 10.31979/mti.2021.2048

Mineta Transportation Institute
College of Business
San José State University
San José, CA 95192-0219

Tel: (408) 924-7560
Fax: (408) 924-7565
Email: mineta-institute@sjsu.edu

transweb.sjsu.edu/research/2048

ACKNOWLEDGMENTS

Funding for this research was provided by the State of California SB1 2019/2020 through the Trustees of the California State University (Agreement # ZSB12017-SJAUX) and the California State University Transportation Consortium. The authors thank Editing Press for editorial services, as well as MTI staff.

CONTENTS

| | |
|------------------------------------|----|
| List of Figures | vi |
| Executive Summary | 1 |
| I. Background..... | 2 |
| II. Numerical Investigations | 4 |
| 2.1 Numerical Model..... | 4 |
| 2.2 Numerical Simulations | 6 |
| III. Results and Discussion | 7 |
| 3.1 Closed Door..... | 7 |
| 3.2 Open Doors | 15 |
| 3.3 Analytical Results..... | 22 |
| IV. Conclusion..... | 27 |
| Endnotes | 28 |
| Bibliography..... | 30 |
| About the Authors..... | 32 |

LIST OF FIGURES

| | |
|---|----|
| Figure 1. The Commuter Bus with Seated Passengers (2pp.) | 4 |
| Figure 2. Pressure Probes for Grid Dependency Test and the Infectious Passenger | 6 |
| Figure 3. Contours of Mean Velocity | 8 |
| Figure 4. Contours of Mean Pressure | 9 |
| Figure 5. Particles' Dispersion | 10 |
| Figure 6. Particles' Dispersion, Longer Duration | 11 |
| Figure 7. Contours of Axial Vorticity | 13 |
| Figure 8. Contours of Turbulent Kinetic Energy (TKE) | 14 |
| Figure 9. Contours of Mean Velocity (2pp.) | 16 |
| Figure 10. Contours of Mean Pressure (2pp.) | 18 |
| Figure 11. Particles' Distribution (2pp.) | 20 |
| Figure 12. Contours of Vorticity (2pp.) | 23 |
| Figure 13. Contours of Turbulent Kinetic Energy (TKE) (2pp.) | 25 |

Note: “2pp.” in a figure title indicates that the relevant figure spans two pages

Executive Summary

Among the major health concerns due to the COVID-19 pandemic is the spread of viruses aboard public transportation systems from infected passengers. Spreading of viruses and bacteria due to coughing, sneezing, sudden release of an agent, or just breathing normally within the public transportation systems with high people to space concentrations is also of high concern for homeland security. One of the unresolved issues in addressing contaminant impact is the pathogen's residence time, considering other local environmental conditions such as the indoor air flow and passenger movements. Another issue is the impact of social distancing and mask usage on virus transport and infection rate. Our recent investigations¹⁵ of virus transport aboard a commercial plane have shown that wearing a mask, social distancing, and a high ventilation rate are effective measures to reduce the spreading rate and the virus's residence time and thus improve environmental health.

Here we provide results of our unsteady numerical investigations of virus transport when particles are released aboard a commuter bus with 37 passengers from an infectious passenger sitting in the middle of the bus. The simulations include the impact of air exchange due to the opening and closing of the bus's middle door during a bus stop. The study aimed at understanding the risk of infection to other passengers from the release of viruses from a single source during the sedentary condition; 2.5-micron particles were used to simulate aerosolized viruses. The study assumed 1,267 particles/min were released from an infectious passenger. The numerical results indicate a high risk of infection for passengers sitting adjacent to and behind the infectious person when the bus is in transit and a high exposure rate for the passengers sitting in front of the infectious person when air exchange occurs at the bus stop. However, the estimated risk of infection is low for 30 minutes of exposure.

I. Background

The speed of air emitted from coughing and sneezing could reach 100 MPH with an excess of 100,000 bacterial particles, including up to 40,000 droplets released from the nose and mouth. Viruses and bacteria and the aerosols that contain them have different sizes. The typical diameters for bacteria are 0.1–0.5 microns, and flu viruses are 0.002–0.4 microns in diameter. The influenza virus is about 0.1 microns, and pneumonia, which is from bacterial infection, has an average size of 0.25 microns. Measles, flu, and chickenpox viruses are about 0.12, 0.22, 0.3 microns, respectively.

Previously we have performed unsteady numerical simulations of the release of droplets/particles from coughing passengers seated at windows or aisle seats.¹ The objective of the study was to understand how the viruses were dispersed within a commercial regional aircraft cabin and to determine the residence times for these viruses for passengers seated in front, adjacent, and behind the coughing passengers. Results indicated that rear row passengers are not significantly affected by the coughing; however, there were significant exposures for passengers seated adjacent and in front of the coughing passenger. The levels of exposure for these passengers (their residence time) were initially higher when the coughing passenger was at the window seat which indicated that the wall effects and shear might have played a role in retaining the viruses resulting in increased residence time for the exposed passengers.

Published investigations have shown that the spatial distribution of airborne pathogens is one of the most important factors in infection risk assessment for respiratory diseases.^{3, 4, 5, 6, 7, 8, 9} Wells-Riley (WR) and Dose-Response (DR) methods have been used to estimate the risk of infectious respiratory diseases. In the WR approach the focus is only on the airborne route from a single source strength, while in DR, in addition to the airborne route, other transmission routes such as surface contamination and virus survival are also considered. This approach includes the source strength and the quantity of the pathogen in its estimation. Factors impacting the airborne transmission of pathogens include its dispersion and distribution within the indoor environment, aerosol size, respiratory deposition, air turbulence, control measures, ventilation strategy, pathogen-host interaction, and survival of the pathogen.³

The WR equation evaluates the probability of infection, considering the intake dose of airborne pathogens in terms of the number of quanta (a single quantum is a single infectious particle). It assumes steady-state infectious particle concentration that varies with ventilation rate within a well-mixed room.

The equation is defined as:

$$\frac{n}{N_s} = \left(1 - e^{-\frac{n_0 q_n Q_B t}{Q_r}} \right) \quad (1)$$

Here, n is the number of infectious cases, N_s is the population, n_0 is the number of infectors, q_n is the quanta generation rate (quanta/minute), t is the exposure time in minutes, and Q_B and Q_T are respectively the person's and the room's ventilation rates in cubic feet per minute (CFM).

Recent modeling of aerosolized virus concentration⁴ based on experimental data from occupants assuming clean air free of the virus entering an enclosure (a room) has shown that the virus emission rate is $1.6 \pm 1.2 \times 10^5$ genome copies/m³h. Measurements of virus-laden aerosols in infectious breath⁵ showed a virus generation rate (q_g) of 1,267 viruses/minute (or copies/minute). The corresponding virus infectivity (copies/quanta) with human 50% infectious dose (HID₅₀) for these cases investigated was 2,554 copies/quanta. The quanta generation rate, q_n is calculated as:

$$q_n = \frac{q_g}{\text{copies/quanta}} = 0.645$$

Equation 1 can be written as:

$$\frac{n}{N_s} = 1 - e^{-\left(C / \frac{\text{copies}}{\text{Quanta}}\right) Q_B t} \quad (2)$$

$$(C = \frac{n_0 q_g}{Q_T} = \text{inhaled concentration, virus/ft}^3)$$

Thus knowing N_s and the parameters on the right-hand side of equation 2, the number of infectious cases, n , could be estimated.

The study aimed at understanding the details of spatial transient concentration of the viruses aboard a commuter bus along with passenger exposure to identify the probable number of infections for a specific duration. However, it is important to note that the rate of inhaled particles and deposition in passengers depends on the characteristics of the particles (size, density, shape), the structure of each person's respiratory tract, and the passengers' breathing pattern. There is a high correlation between regions of high wall shear stress, secondary flow, and vortices with particles' deposition.^{10, 11, 12, 13, 14} Obstructions in the respiratory system impose pressure force on the flow field, leading to increased depositions before and after the obstruction.

The study also investigates the effect of air exchange on virus concentration and exposure rate.

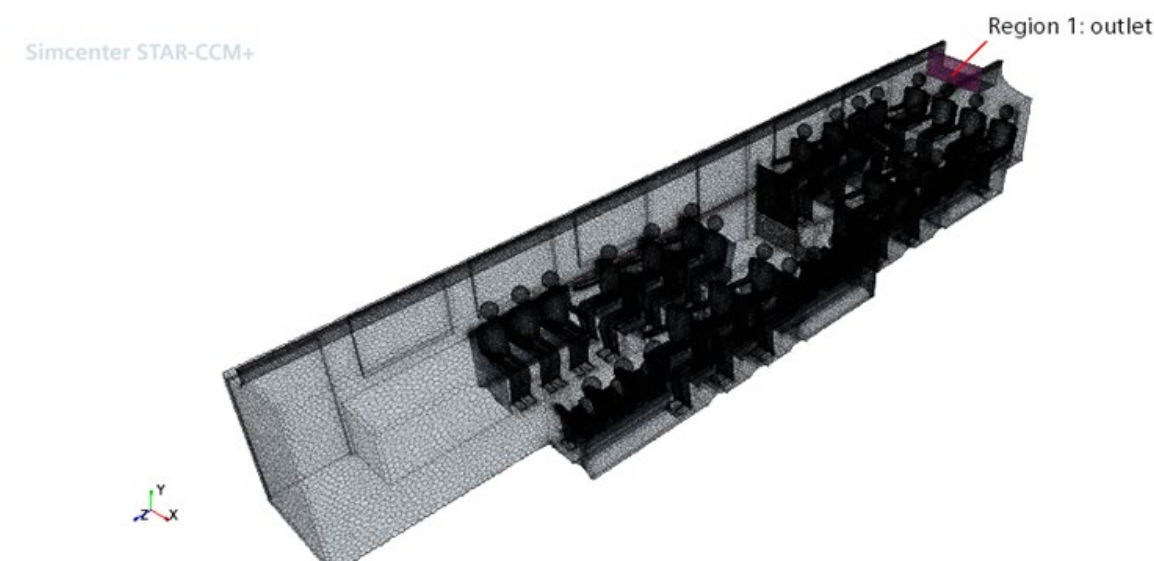
II. Numerical Investigations

2.1 Numerical Model

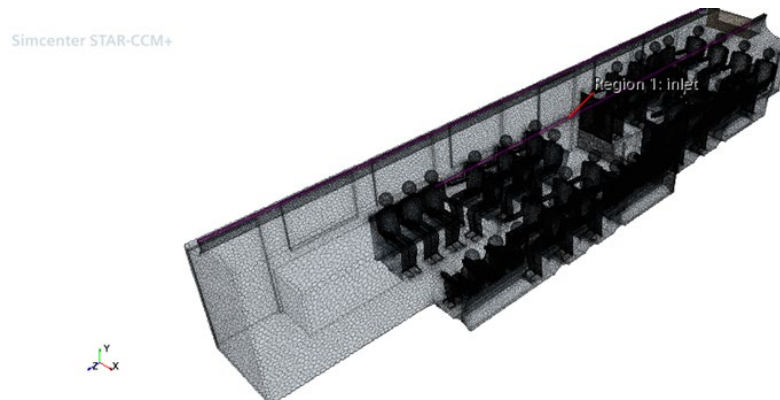
A standard commuter bus with 37 seats fully occupied has been modeled. Figure 1 shows the bus model with seated passengers. Its dimensions are 12.82 m in length, 2.4 m in width, and 2.53 m in height. The dimensions of the bus for constructing the model were taken from an actual transit bus used by the Long Beach Transit (LBT) company. This is an older version of the commuter bus with two linear slots in the ceiling delivering air inside which is exhausted through the back grille (Figure 1d). The airflow is uniform at 1 m/s through two linear ceiling slots with a total volume flow rate of 59.38 m³/min (2,097 CFM). In Figure 1b, region 1 inlet is identified. This is a passenger drop-off door which was left open to the outside for 30 sec when the simulations were performed to represent air exchange with outside during a bus stop. Figure 1c shows the monitoring planes from seated passengers.

Figure 1. The Commuter Bus with Seated Passengers (2pp.)

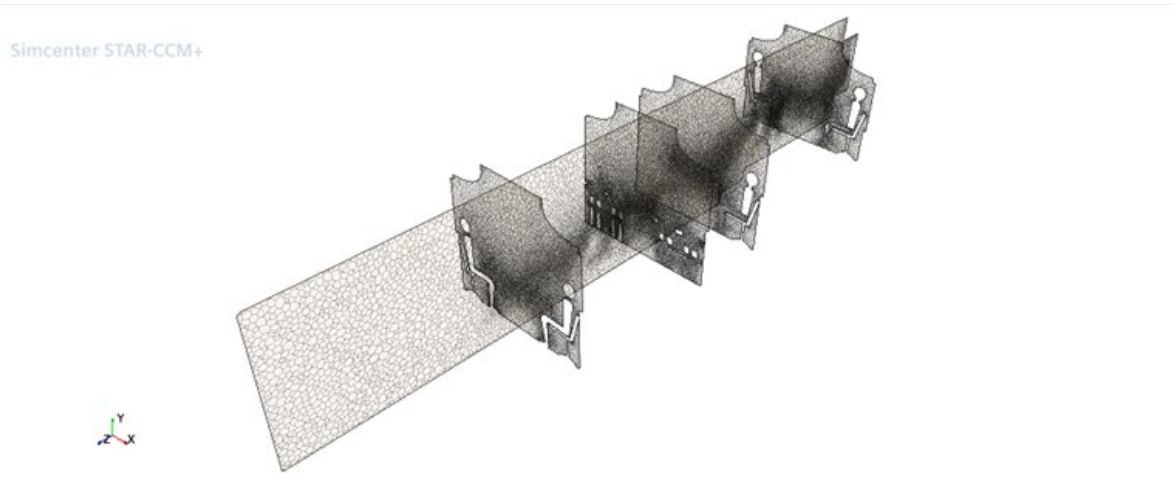
(a)



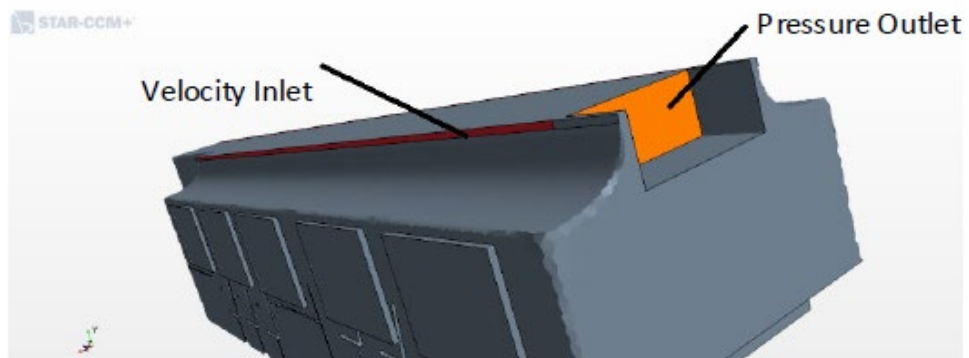
(b)



(c)



(d)

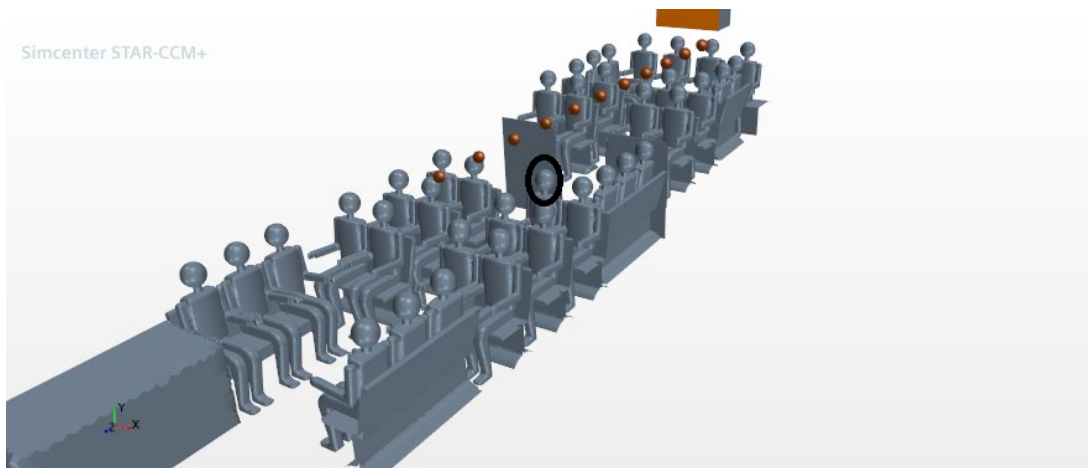


2.2 Numerical Simulations

Three-dimensional incompressible unsteady Reynolds-Averaged Navier-Stokes (U-RANS) equations were solved, using the shear stress transport (SST) $k-\omega$ turbulence model. The computational fluid dynamics software Star CCM+ from Siemens was used on a Linux-based high-performance computing platform with 84 cores for all simulations. Between 150–220 hours of computational time was used for each simulation and the results presented here begin 30 sec after the start of each simulation with a time step $\Delta t = 1$ sec.

Mesh dependency test was performed at time 30 sec (this is the time after the start of the simulation when the particles were released). Since a particle's drag characterizes its movement, variation in pressure was used as a way to finalize the grid size for simulations. Figure 2 shows the location of ten line-probes used for pressure measurements.

Figure 2. Pressure Probes for Grid Dependency Test and the Infectious Passenger



The polyhedral mesh was used for all simulations. The grid dependency test was performed for three meshes of 8.9 million, 12.1 million, and 29.2 million. The maximum percent difference between 8.9 and 12.1 million meshes was 2% and between 12.1 and 29.2 million meshes it was 3%, and thus 12.1 million mesh was used in all simulations.

Figure 2 also shows the infectious passenger in the middle of the bus seated in an aisle seat; 2.5- μm round carbon particles were used to simulate an aerosolized virus without evaporation. The mouth velocity was 0.278 m/s corresponding to 0.3 CFM. The particles' release rate was 21.1 particles/sec or 1,267 particles/min.

III. Results and Discussion

3.1 Closed Door

Figures 3 and 4 show contours of mean velocity and pressure at the mid-section plane and monitoring planes at a 15-sec interval. The results are presented 30 sec after the start of the simulation, to prevent any error associated with the initial developing flow. Air is injected into the bus through the linear ceiling slots. As it moves around the passengers to exit, it creates areas with a cavity (zero velocity) behind passengers, near the footsteps, and below the exit grille at the back. There are air recirculations in between the passenger rows, but most of the airflow is concentrated at the passengers' head height. It is interesting to note that the current air distribution system lacks the capability for full mixing, and non-uniformity in air circulation could impact the virus capturing and ejection process.

The non-uniformity in the mean velocity results in non-uniformity in mean pressure, where the pressure is high when velocity is low and vice versa. At 30 sec, the pressure is nearly uniform around the infected passenger. At 45 sec, lower mean pressure is observed around the passenger's head, starting from the first horizontal row that expands to the back of the bus. This is the area where the air is moving effectively. With the increase in time, the variations of the mean pressure with time indicate the impact of blockage and distortion on mean velocity and pressure, which should impact the spatial virus concentration with time.

Figure 5 shows the time variation of particle (virus) diffusion within the bus. At 30 sec, the viruses are released from the infectious passenger and are then picked up by the inside ventilation air and dispersed within the bus. At 45 sec, the adjacent passenger is exposed. At 60 sec, there are diversions of some particles toward the passengers seated right behind the infected passenger and the next row, and the particles, in general, are moving with the air in the middle toward the back seats. At 75 sec, there is a large concentration of particles facing the passenger sitting behind the row where the infectious passenger is sitting. At 90 sec, concentrations in the other rows have decreased while a significant number of particles were released from the infected passenger.

Figure 6 shows particle concentration for longer durations of 10, 20, and 30 minutes. Reviewing these concentrations, the exposure risks are highest for passengers sitting adjacent to and behind the infectious passenger.

In conducting our simulations, we assumed non-stick boundary conditions for the particles, where they bounced from the surfaces upon impact and have the tendency to remain within the air stream. For aerosolized viruses, this might not be true, as in general, with evaporation, the virus size becomes much smaller and particles tend to deposit to nearby surfaces with increased deposition velocity aligned with the turbulent diffusion-eddy impaction characteristics.

Figure 3. Contours of Mean Velocity

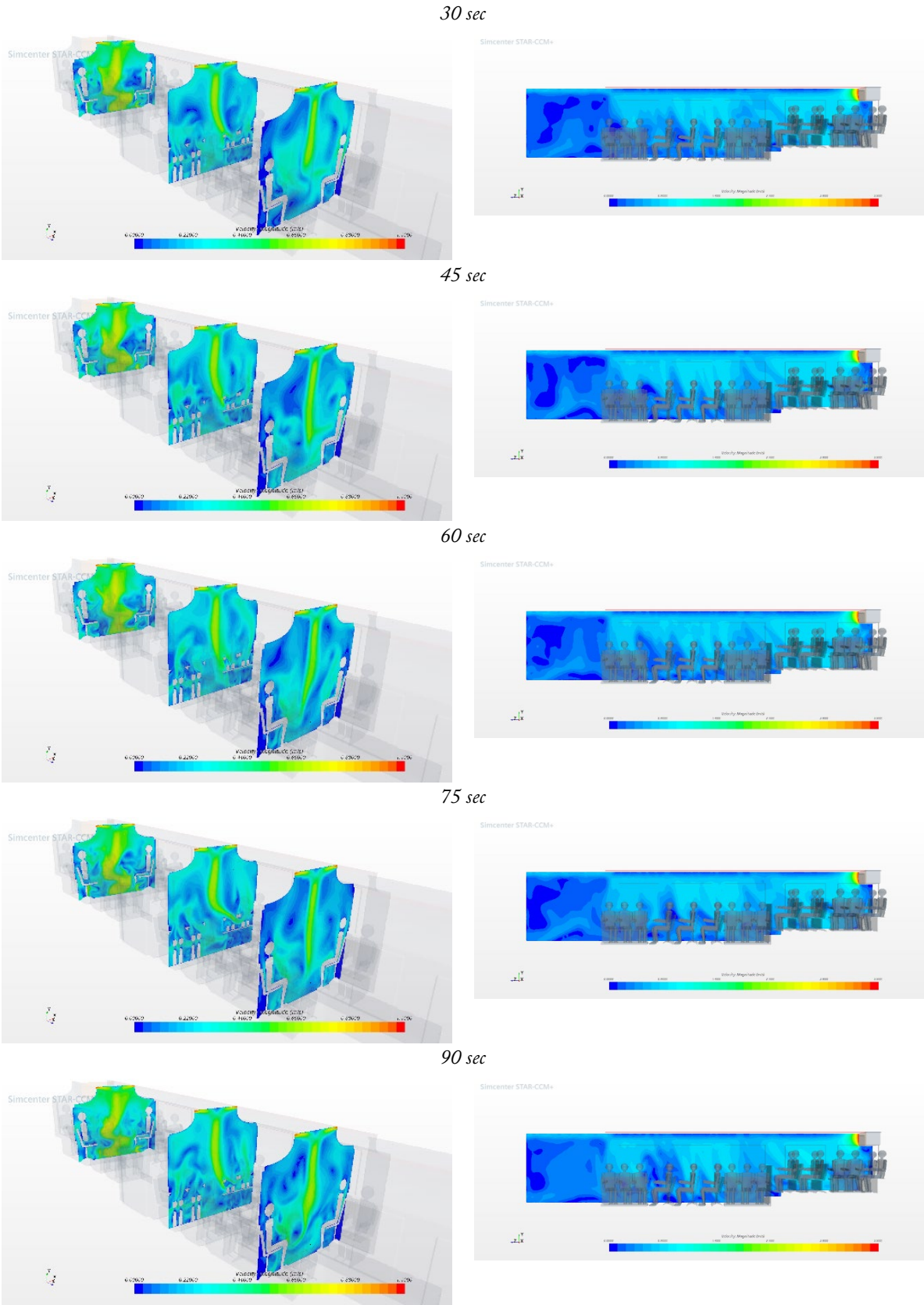


Figure 4. Contours of Mean Pressure

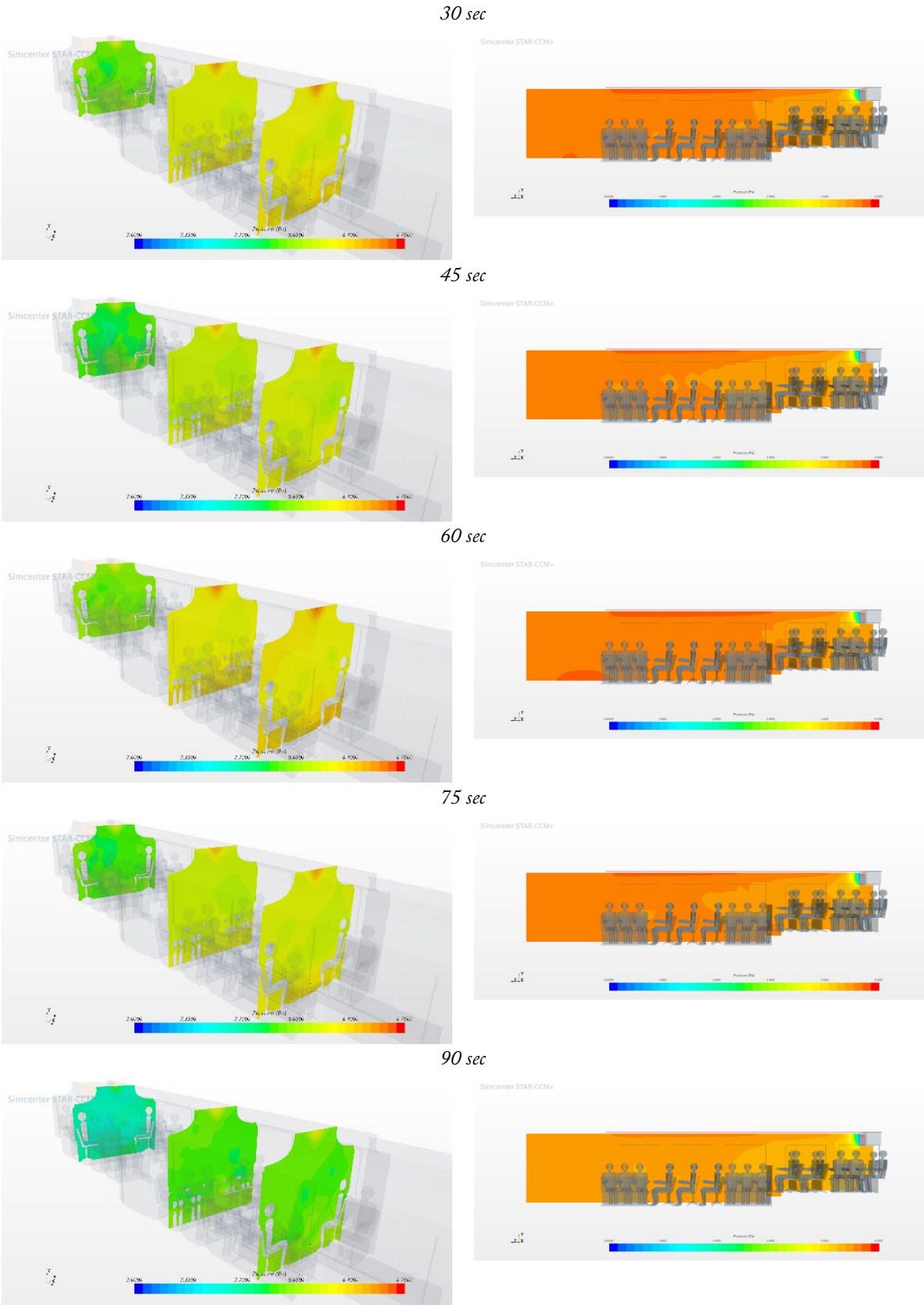
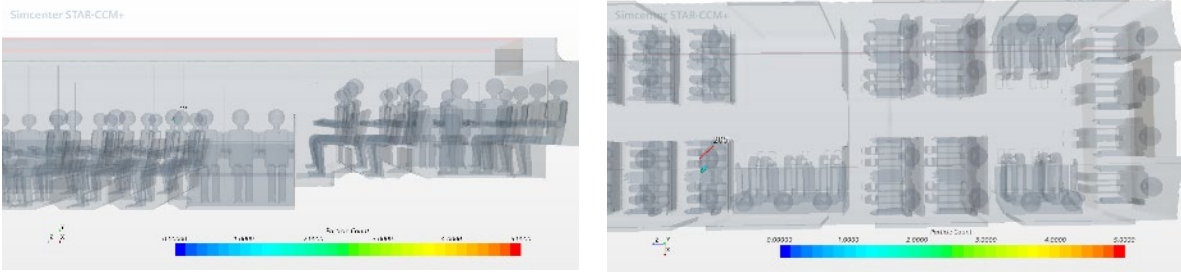
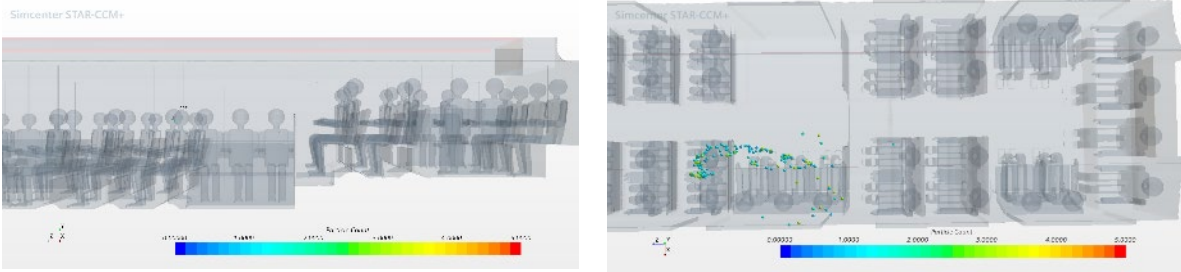


Figure 5. Particles' Dispersion

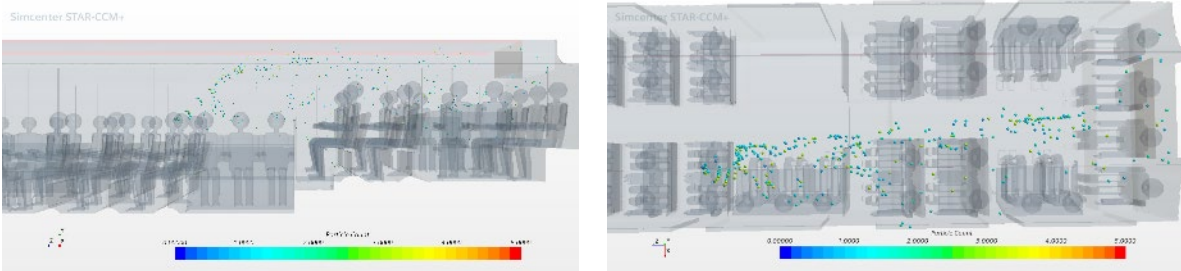
30 sec



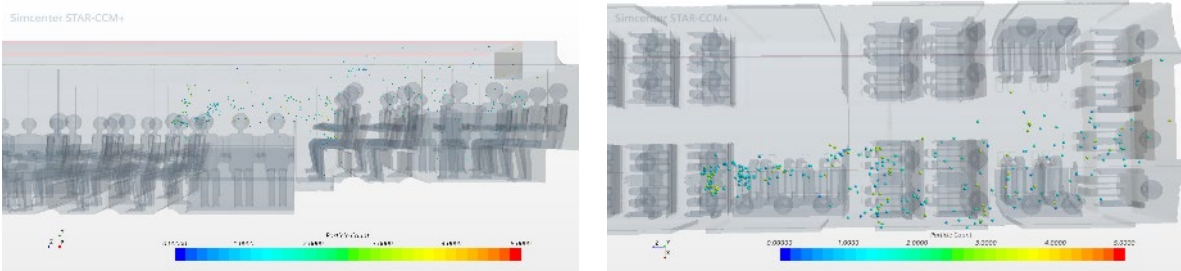
45 sec



60 sec



75 sec



90 sec

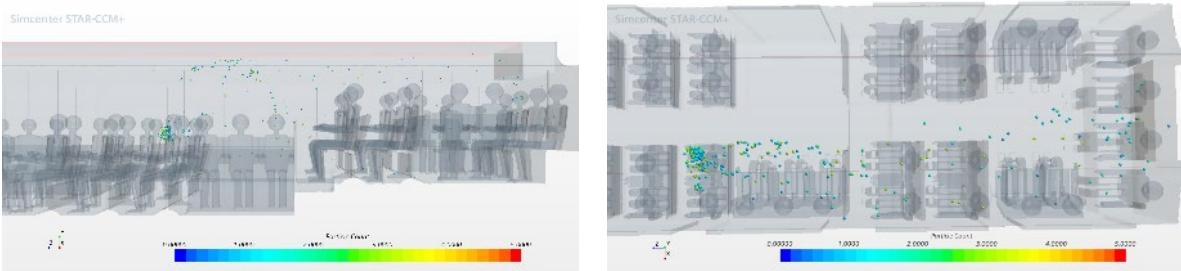
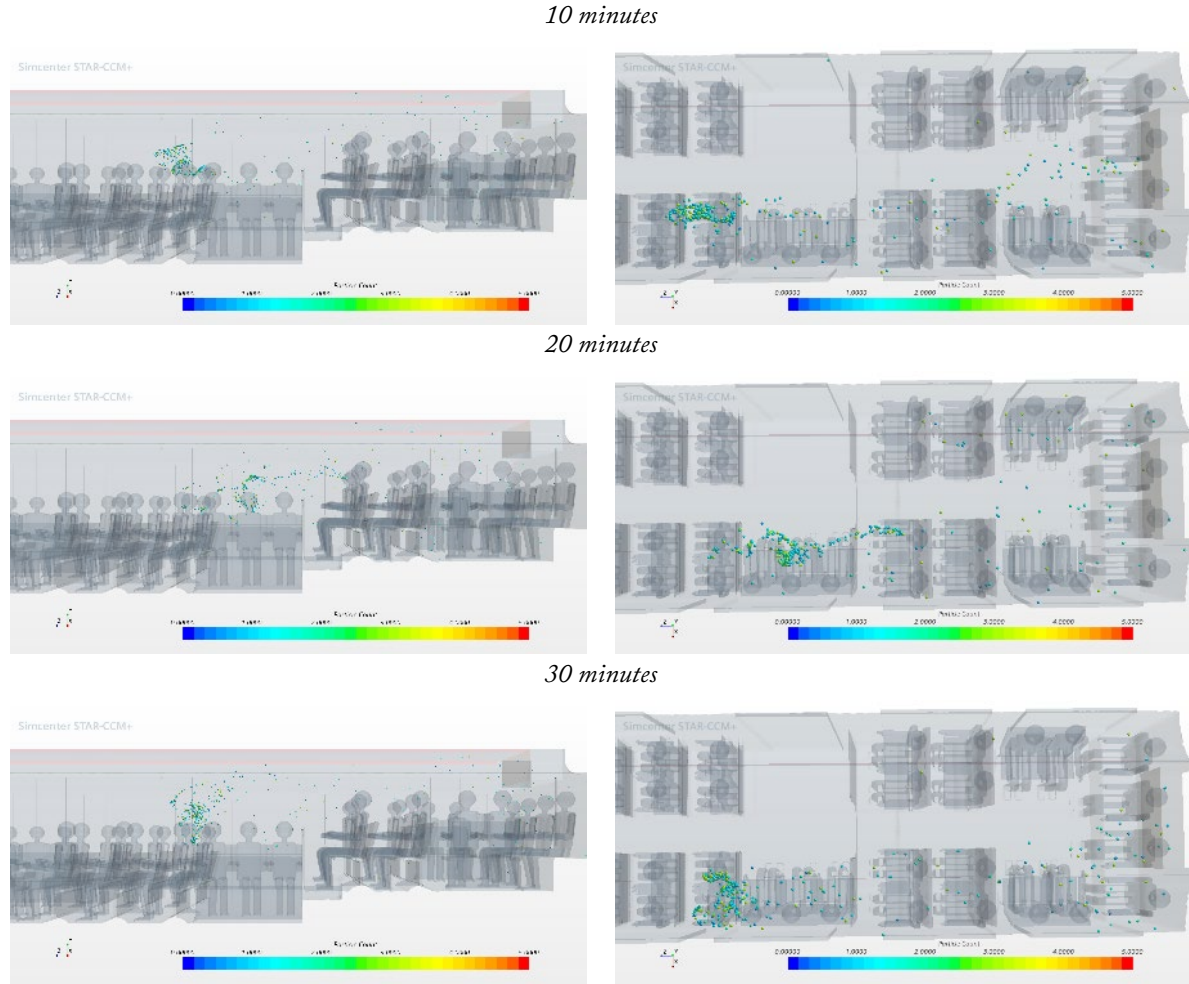


Figure 6. Particles' Dispersion, Longer Duration



Figures 7 and 8 show contours of axial vorticity and turbulent kinetic energy at different time steps. Increased vorticity is observed around the passengers seated toward the back of the bus. Vorticity is the curl of the velocity field defined as:

$$\omega_i = \epsilon_{ijk} \frac{\partial u_k}{\partial x_j}.$$

Here ω_i is vorticity in the i direction, ϵ_{ijk} is the Kronecker- δ , u is the mean velocity, and x is direction. The indices i, j, k are axial, vertical, and spanwise directions, respectively, and summation rules apply. The axial vorticity is then defined as:

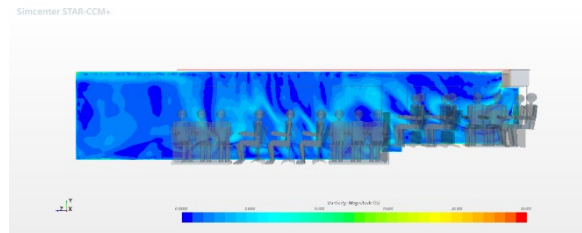
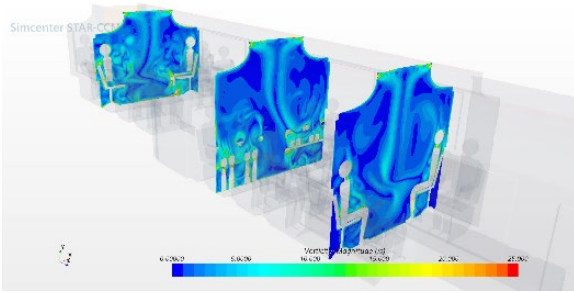
$$\omega_1 = \frac{\partial u_3}{\partial x_2} - \frac{\partial u_2}{\partial x_3}.$$

Increased vorticity is associated with mixing. With ceiling air injected into the cabin at the mid-section, there is reduced air recirculation around the seated passengers, especially toward the back of the bus where the seats are elevated, which reduces particle concentration in these areas. Reducing particle concentration reduces the risk of infection for passengers sitting in the back seats.

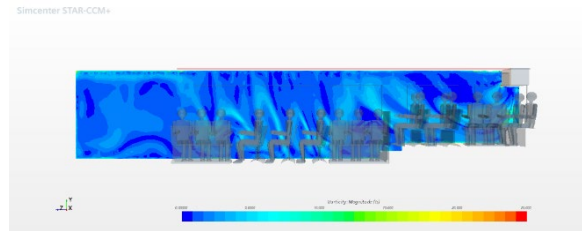
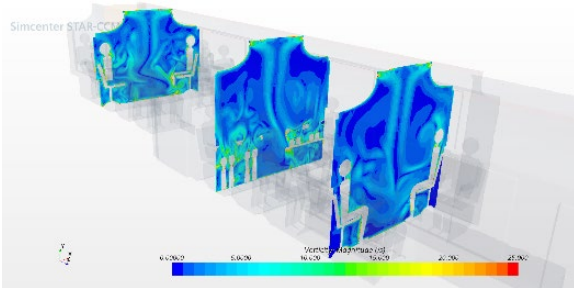
Turbulent kinetic energy (TKE) is associated with the energy of turbulent eddies. Distortion of the air inside the cabin due to non-uniformity (passengers, seats, steps, etc.) generates turbulence, which increases the TKE. Increased TKE is associated with increased mixing. Increased TKE is observed in the row behind the infectious passenger. However, the increase in TKE is contained within the boundary of the air movement. Increased TKE is also observed near the end of the bus, where airflow is diverted toward the exhaust.

Figure 7. Contours of Axial Vorticity

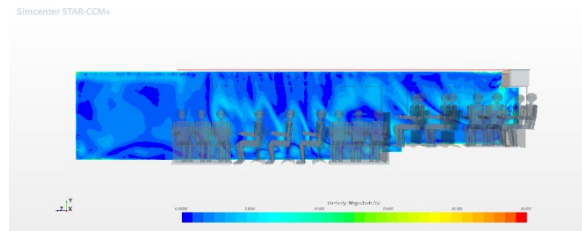
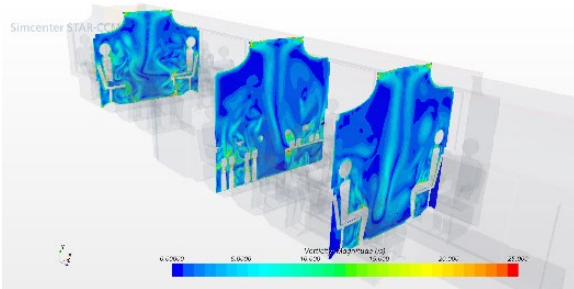
30 sec



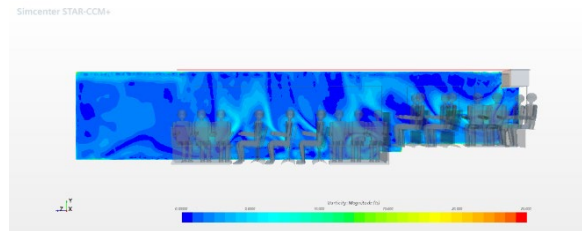
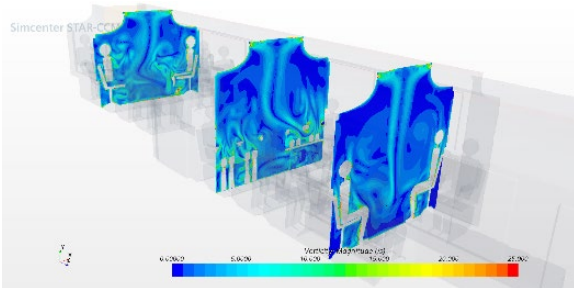
45 sec



60 sec



75 sec



90 sec

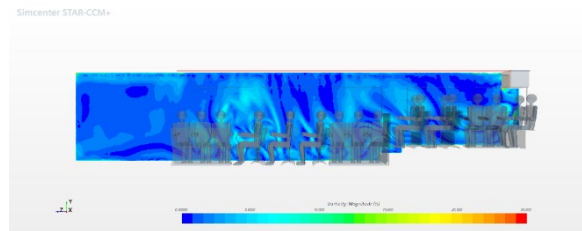
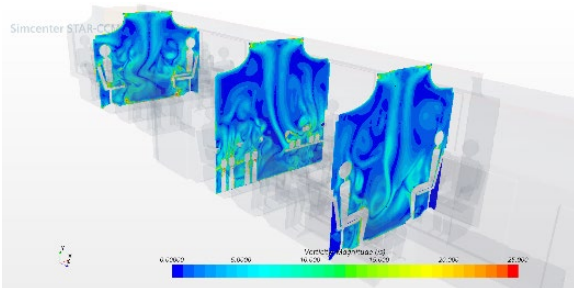
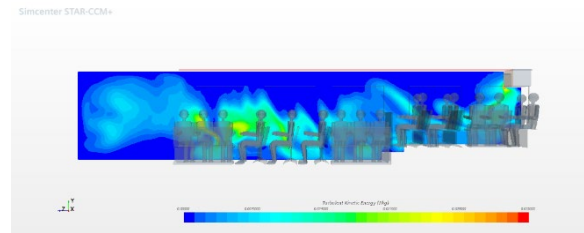
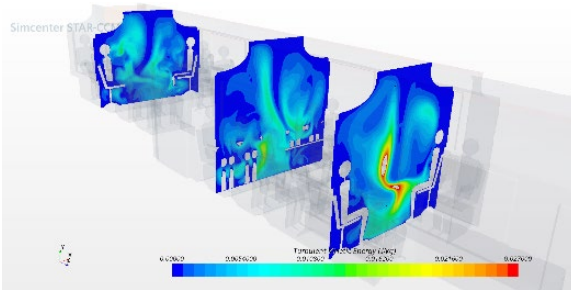
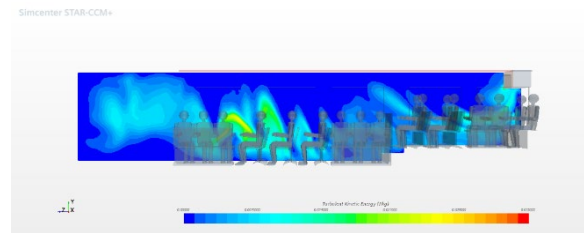
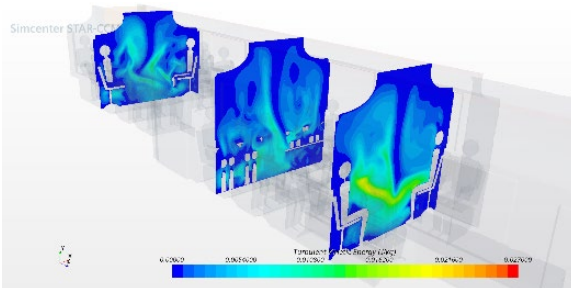


Figure 8. Contours of Turbulent Kinetic Energy (TKE)

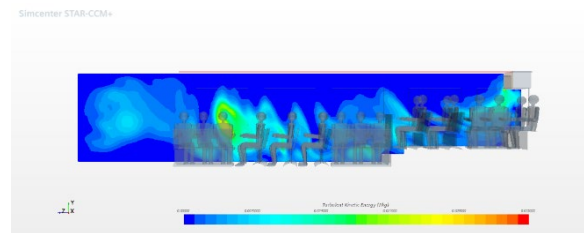
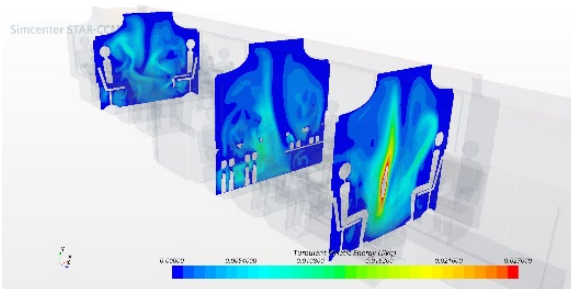
30 sec



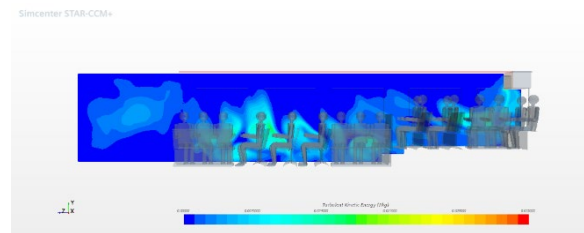
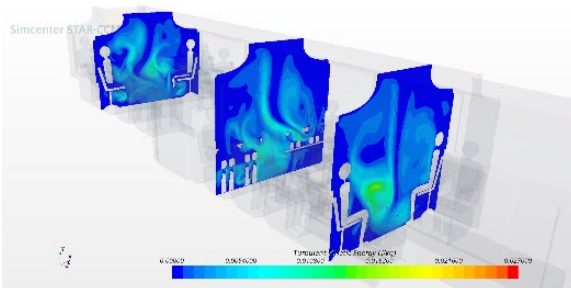
45 sec



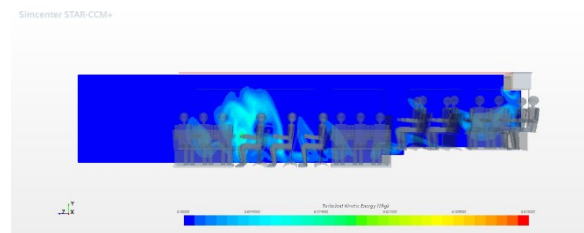
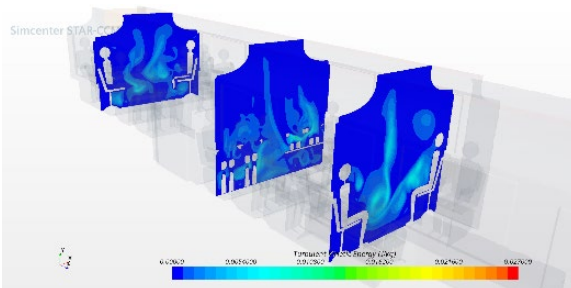
60 sec



75 sec



90 sec



3.2 Open Doors

Figures 9–11 show contours of the mean velocity and pressure and particles' distributions in the following scenarios: at 5 sec before the doors opened, while doors remained open for 30 sec, closed doors, and 30 sec after the doors were closed at different time steps. Here the contours range—for the mean velocity has been changed from 0–3.5 m/se (for the closed-door condition) to 0–10 m/s—to capture velocity variations.

Before the doors open and while they are open, the air movements were toward the back of the bus. However, 5 sec after the doors opened, the passengers sitting in front of the doors experience increased air velocity, and thus results in the subsequent time steps show air movement toward the seats in front of the infectious passenger. When the doors were closed, the outside air intake was stopped, and again the ceiling air moves toward the back exit.

The contours of pressure show moderate pressure distribution before the doors are opened. However, once the door opened, there is a significant drop in pressure moving towards zero gauge pressure, equalizing pressure inside and outside of the bus. Pressure variations are seen at 5 sec after the doors opened, which is the initial stage when the pressure changes to match the outside pressure.

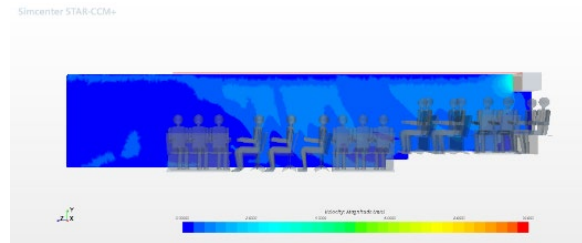
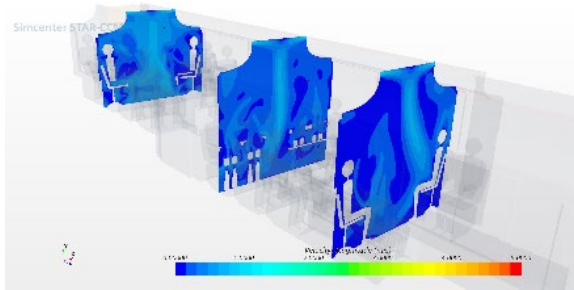
Before the doors opened, the particles' concentration was highest at and around the infectious passenger, traveling with a low concentration on that side of the bus, changing direction near the back toward the middle of the bus to exit. When the doors opened, the rush of the outside air into the bus reduces concentration around the infectious passenger, spreading the particles around, exposing passengers sitting behind the infected passenger. With doors open for the next 30 sec, the particles disperse toward the front row passengers, and some move toward the doors. The dispersion exposes passengers sitting in the two rows in front of the infectious passenger, while the particles' concentration was reduced around passengers sitting immediately behind the infectious passenger.

These dynamics are in line with the distributions of mean velocity and pressure. The air exchange initially reduces inside pressure, causing air within the bus to rush toward the opened doors, which causes similar movements for the pathogenic particles. After this event, there is a movement of the outside air into the bus, resulting in reduced pressure in the front, causing air movement in this direction and thus particles' redistribution toward the front passengers.

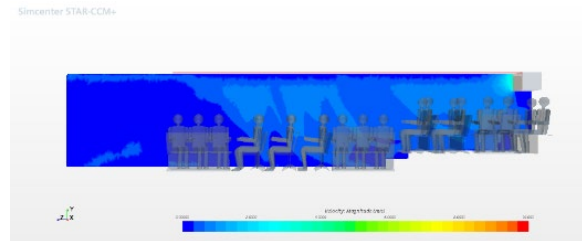
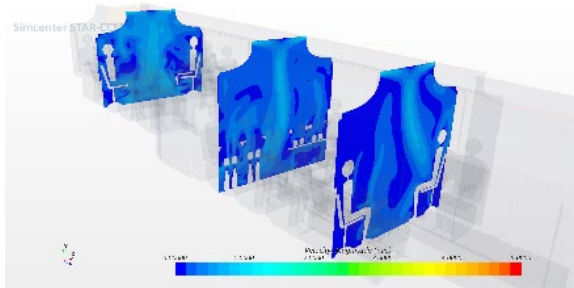
When the doors were closed and air exchange with the outside was stopped, the particles' directions were changed toward the back of the bus, but now particles could reach the passengers on the other side of the aisle, before reaching the back to exit. Contours of mean velocity and pressure for the time steps with closed doors show redistribution of the mean velocity and pressure, with reduced pressure around the passengers on the other side of the aisle resulting in increased velocity and air movement in these areas and thus increased particle dispersion.

Figure 9. Contours of Mean Velocity (2pp.)

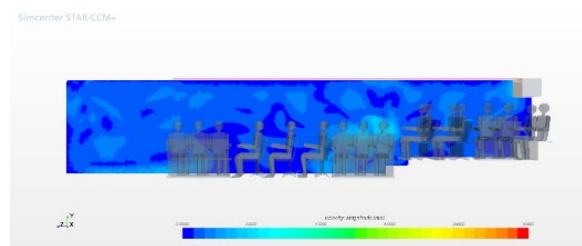
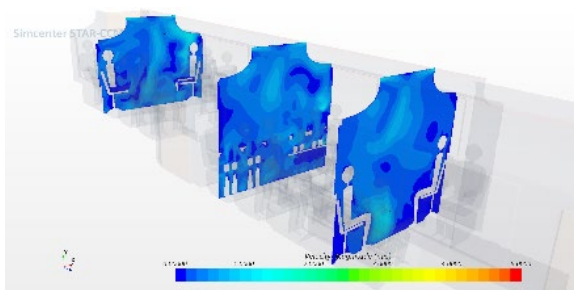
5 sec before doors opening



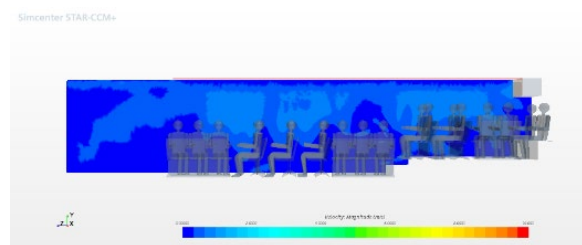
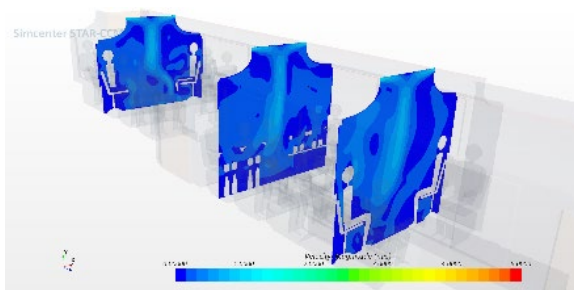
Doors opened



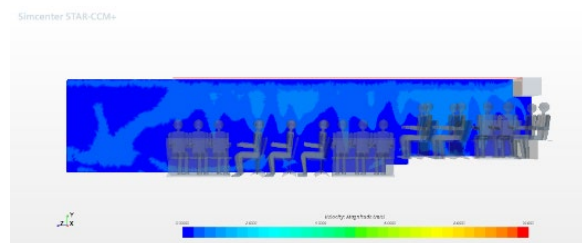
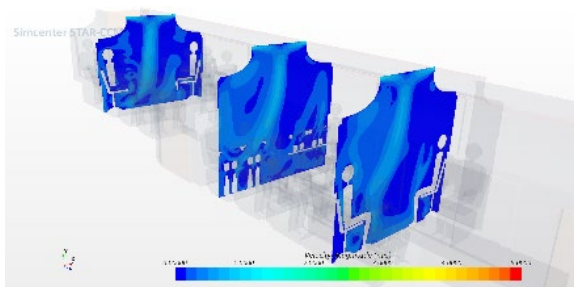
5 sec



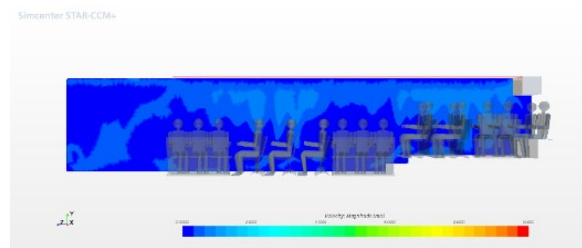
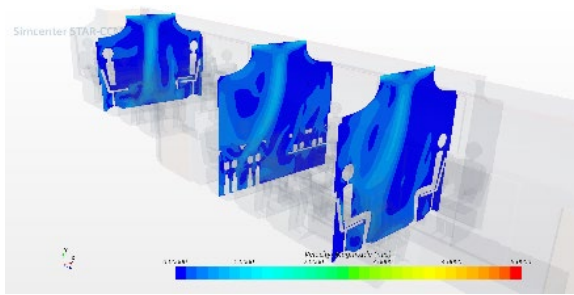
15 sec



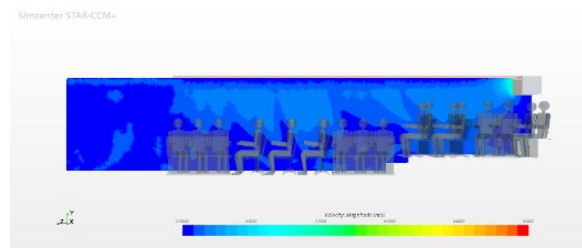
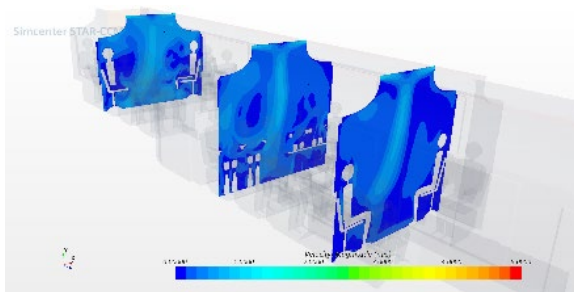
25 sec



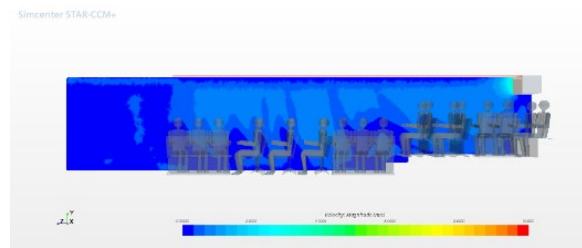
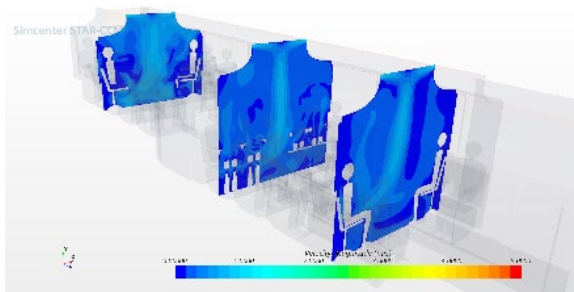
30 sec Doors closed



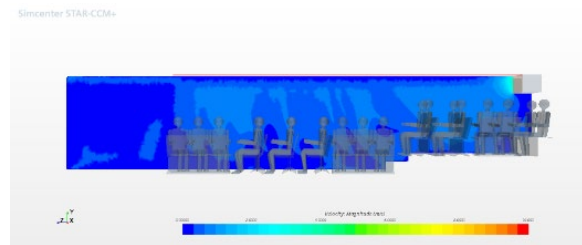
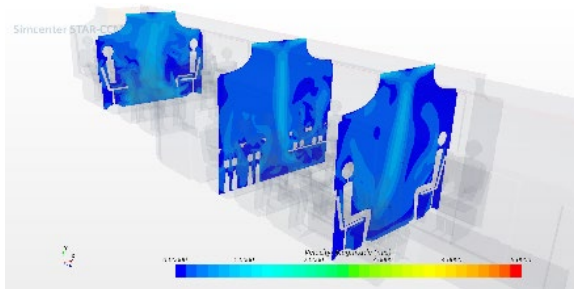
35 sec



40 sec



50 sec



60 sec

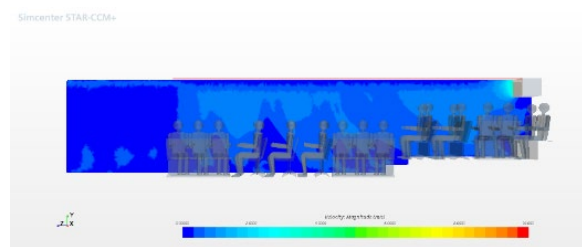
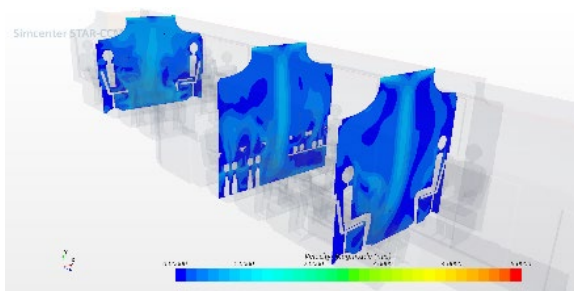
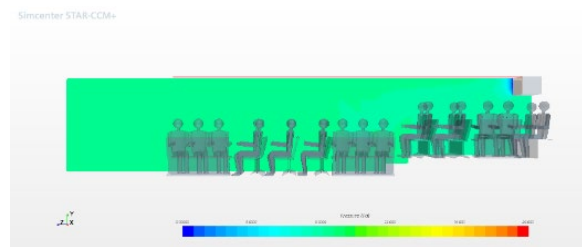
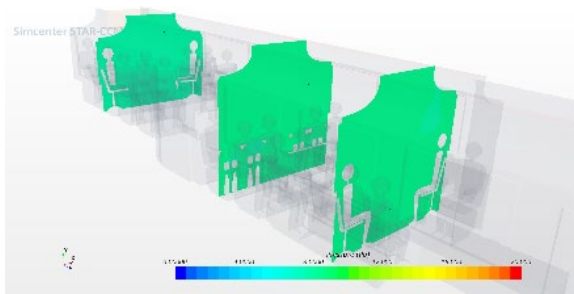
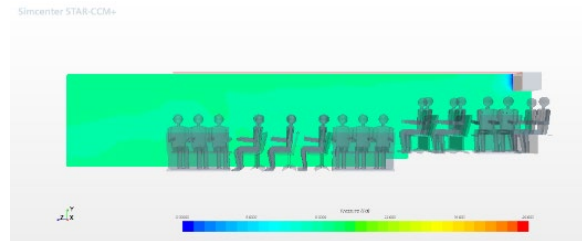
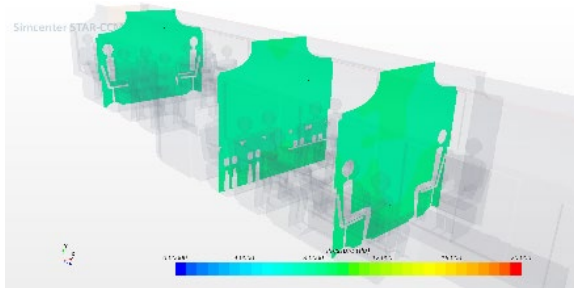


Figure 10. Contours of Mean Pressure (2pp.)

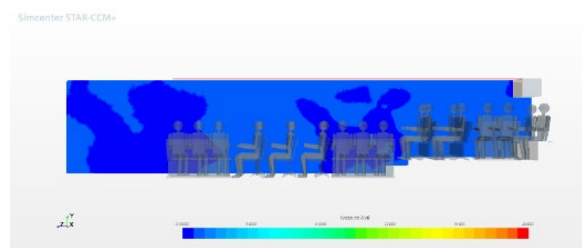
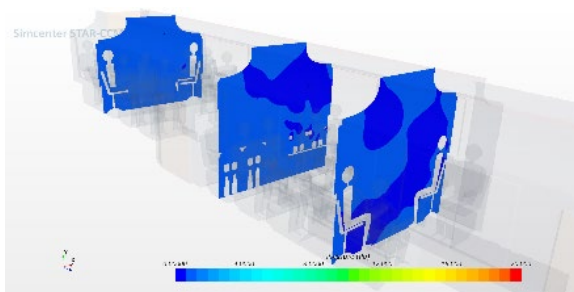
5 sec before doors opening



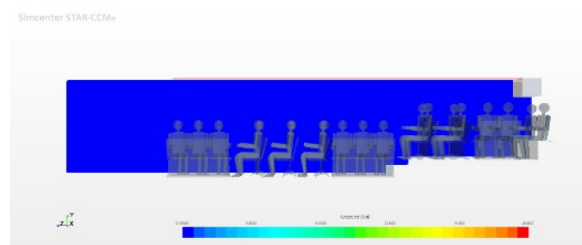
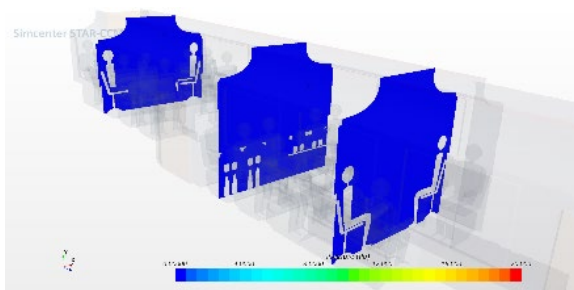
Doors opened



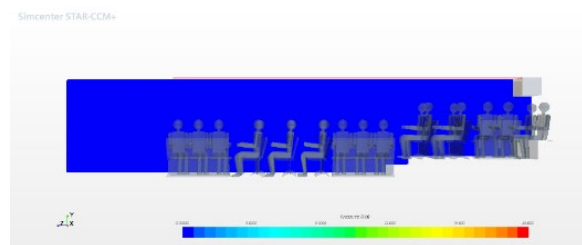
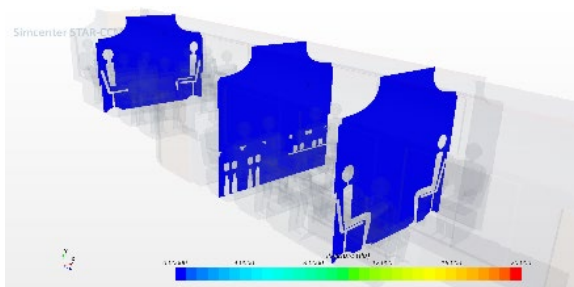
5 sec



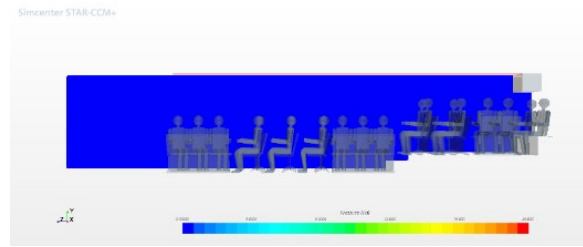
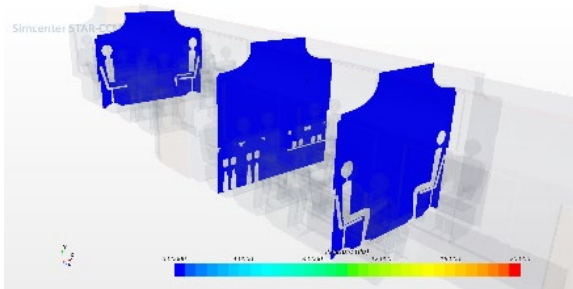
15 sec



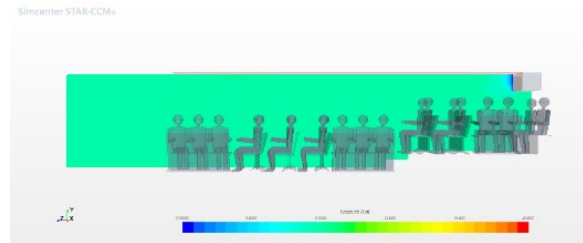
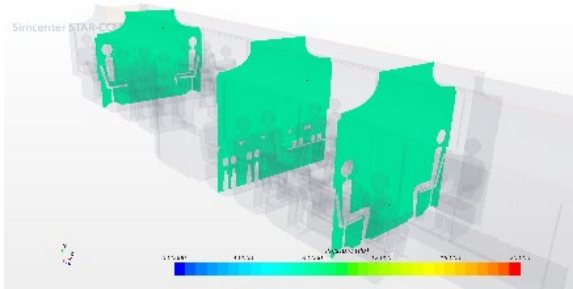
25 sec



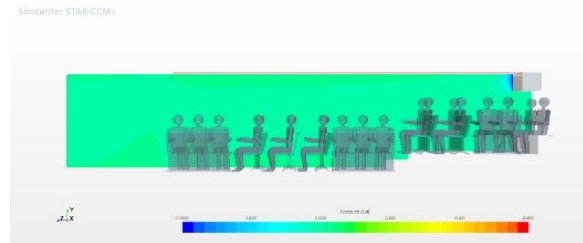
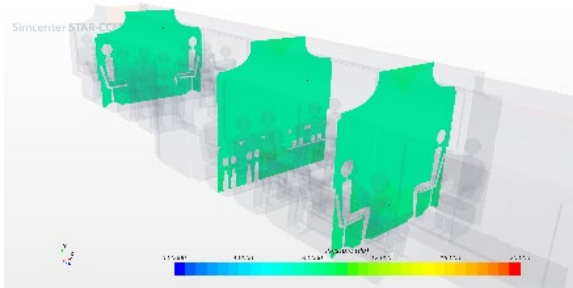
30 sec Doors closed



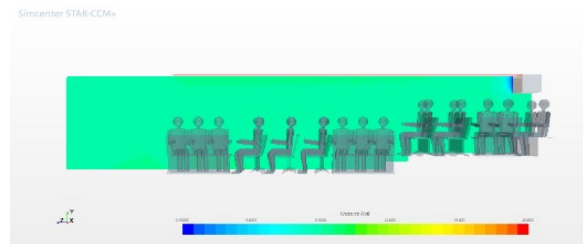
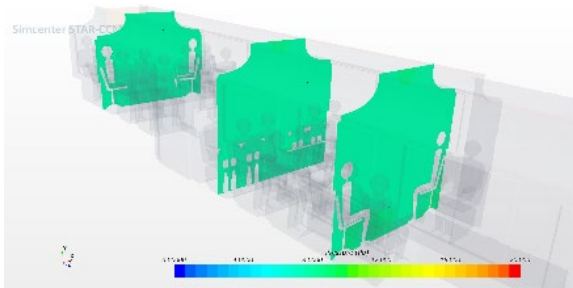
35 sec



40 sec



50 sec



60 sec

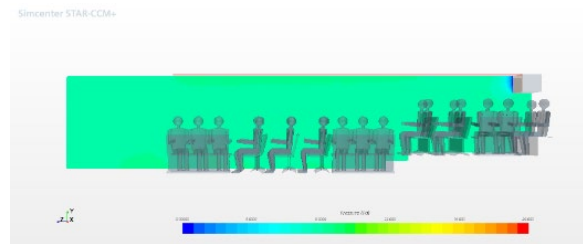
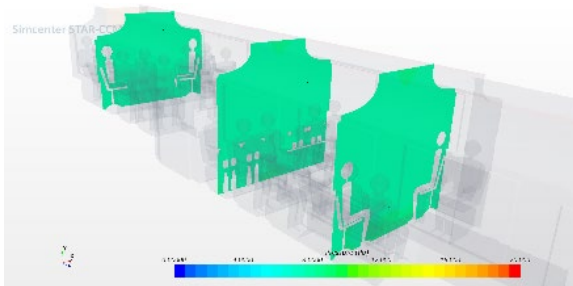
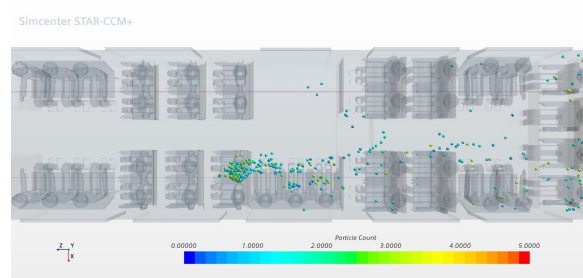
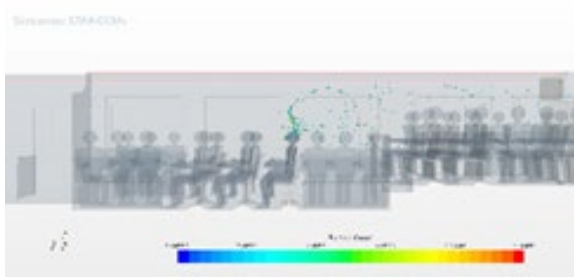
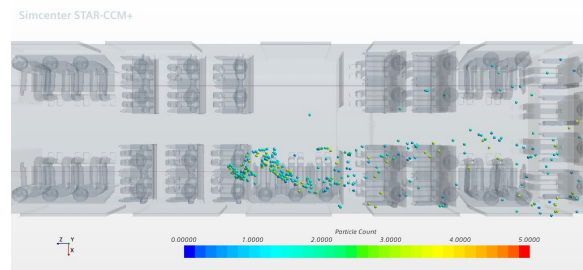
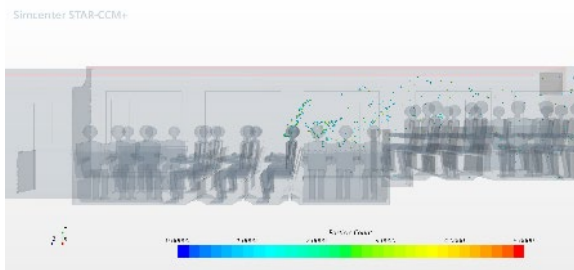


Figure 11. Particles' Distribution (2pp.)

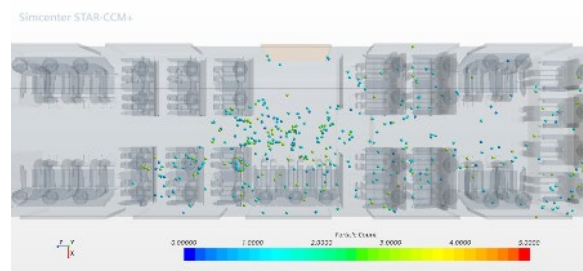
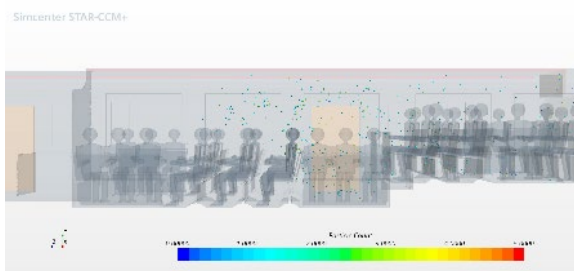
5 sec before doors opening



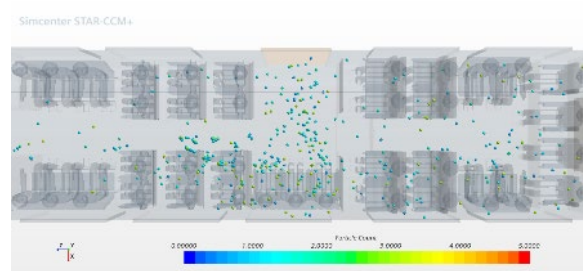
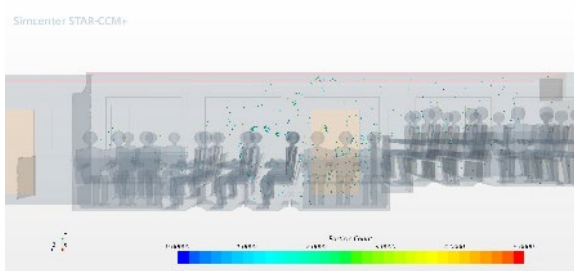
Doors opened



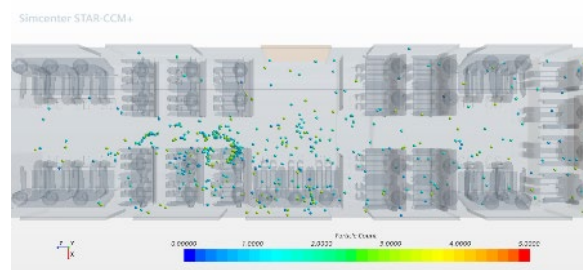
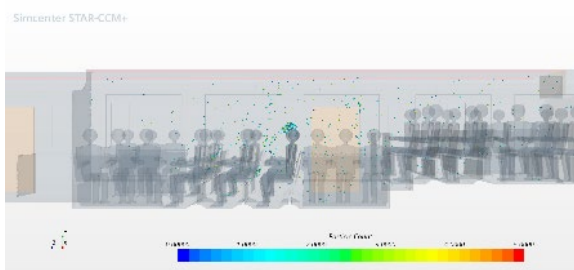
5 sec



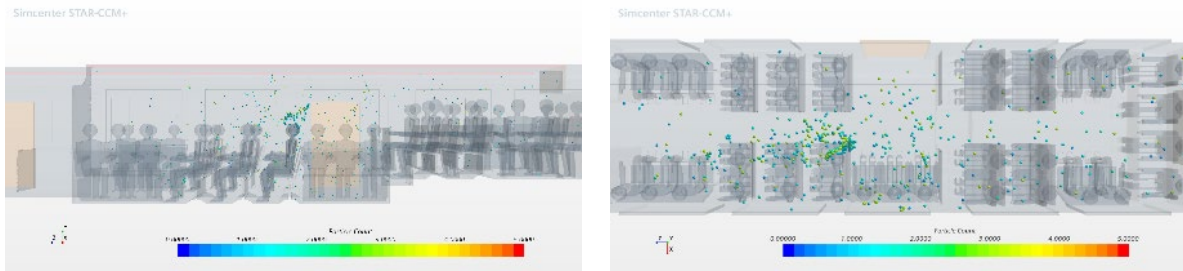
15 sec



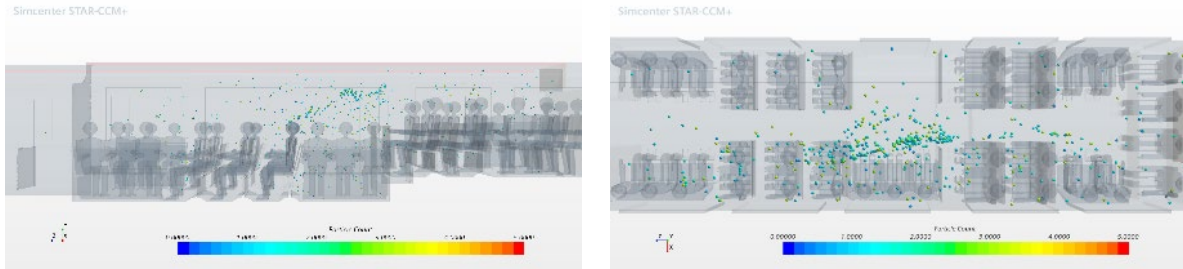
25 sec



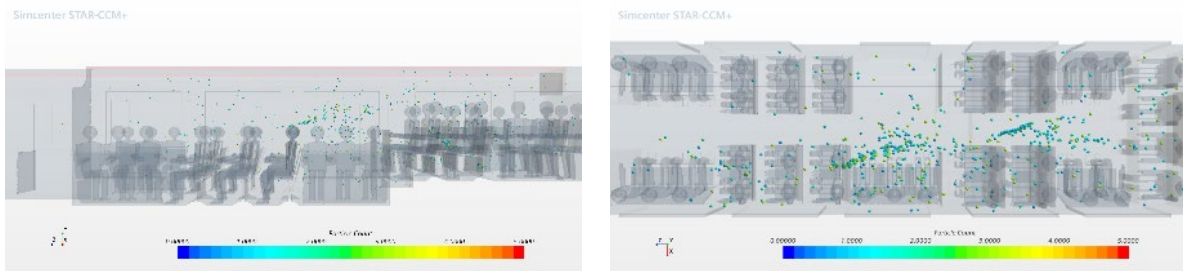
30 sec Doors closed



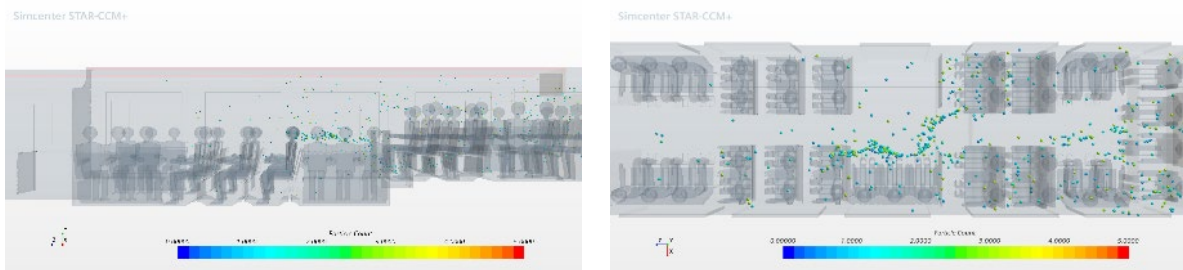
35 sec



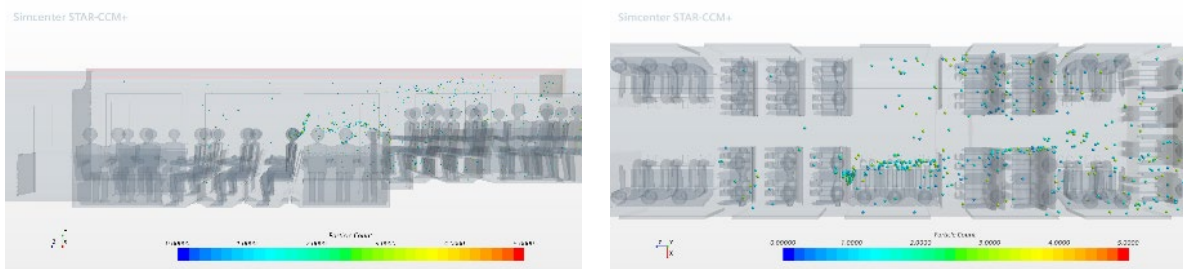
40 sec



50 sec



60 sec



Figures 12 and 13 show the contours of axial mean vorticity and turbulent kinetic energy (TKE). Before and when the doors opened, variations of vorticity were associated with the three-

dimensionalities caused by passengers' distortion, resulting in local velocity gradients and increased vorticity. After the doors opened, the impaction of the outside air on air movement inside the bus results in increased vorticity in areas in front of the doors and near the ceiling, which also causes three-dimensionality in other areas, but the impact is not as significant. However, as time passes and the air exchange is reduced, the vorticity is reduced as well.

When the doors were closed, there is an initial unsteadiness which also results in variations in vorticity. However, with increased time steps, vorticity distribution approaches the corresponding distribution of the condition of the closed doors.

TKE increase is associated with obstruction and impingement. Before the doors opened, increased TKE is observed in rows ahead of the infectious passenger, but after the doors opened, significant increases were observed in areas in front of the door and behind the infectious person which dissipate in time. With the closing of the doors, areas of increased TKE shift from in front of the doors and in the back rows to in front of the infectious person and a few rows downstream.

The increase in vorticity and turbulence results in enhanced mixing which causes the spreading of the particles within the bus, as seen in the particles' distribution graphs.

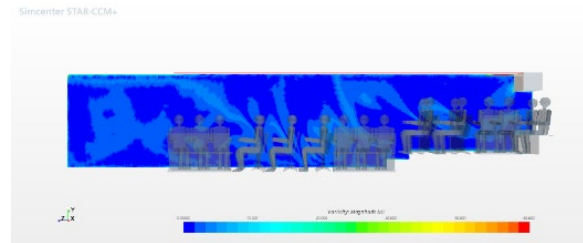
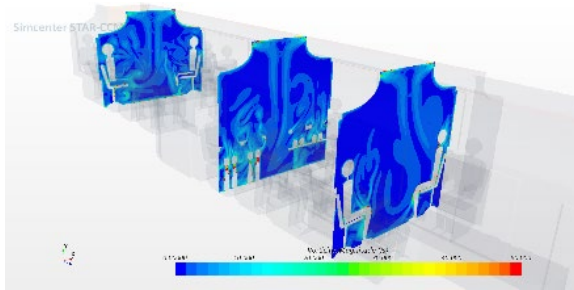
3.3 Analytical Results

Using equation 1 with $q_n=0.645$, for duration 30 minutes, the number of infections would be at 0.11. Because the bus is well ventilated and there is no recirculation, it may take more than 300 minutes of exposure for one passenger to get infected. However, the assumptions for using this equation include having a well mixed air inside the bus which is not the condition of the current simulation. Also, equation 2 offers a better approach if we could measure or estimate copies/quanta for each passenger, which gives us a better estimate of the risk of infection.

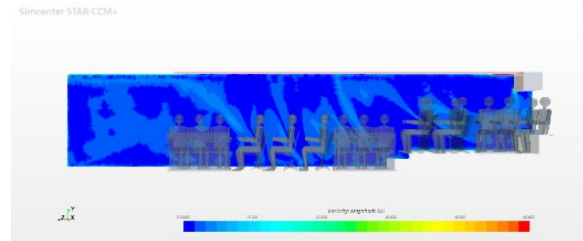
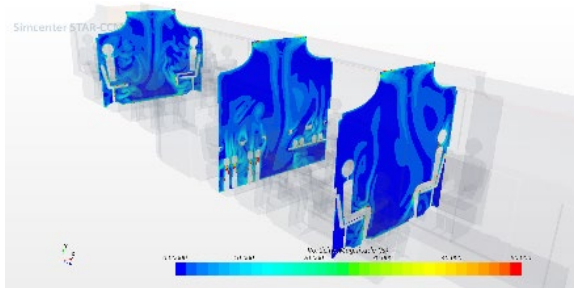
The current simulation is focused on an infectious passenger sitting in an aisle seat in the middle of the bus. Since the air inside the bus is not well mixed, having an infectious person sitting in an area with limited ventilation could increase virus concentration for passengers sitting around the infectious passenger, thus creating a higher risk of infection.

Figure 12. Contours of Vorticity

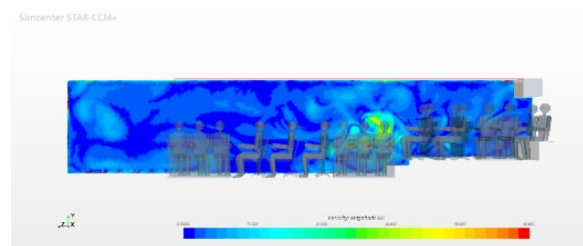
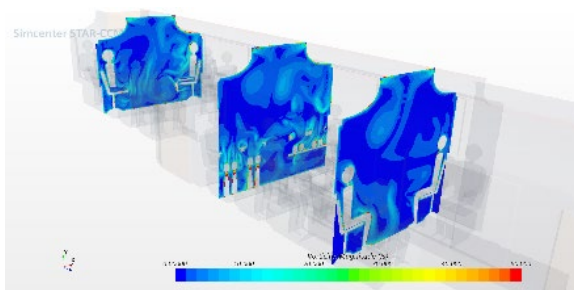
5 sec before doors opening



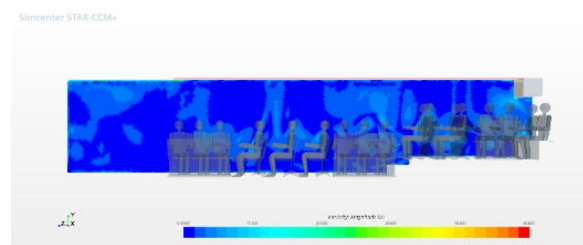
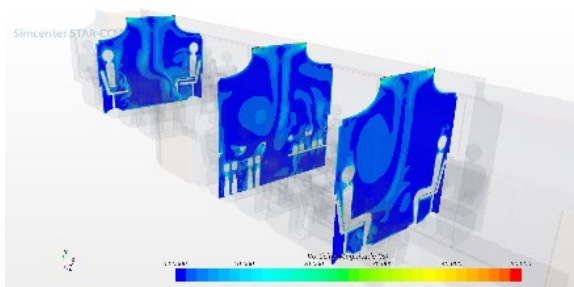
Doors opened



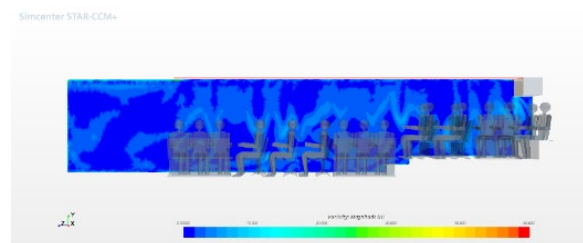
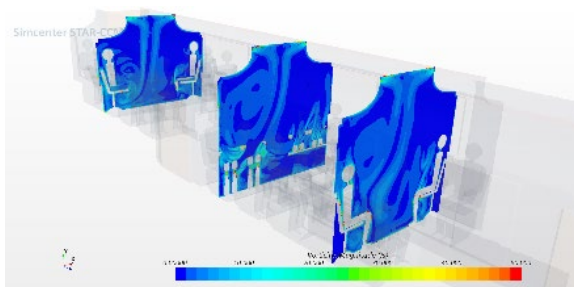
5 sec



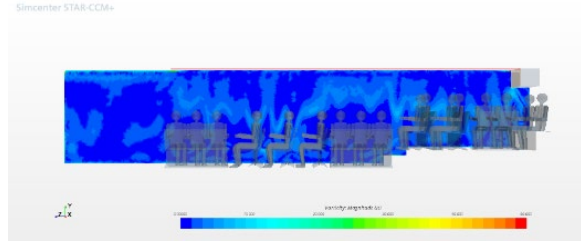
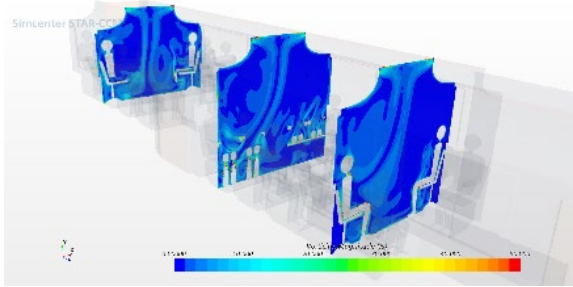
15 sec



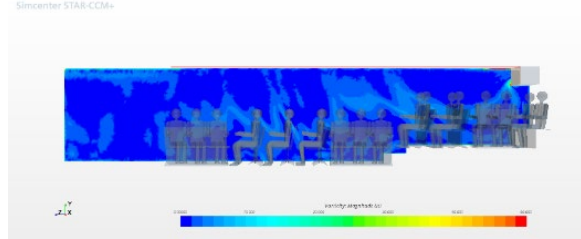
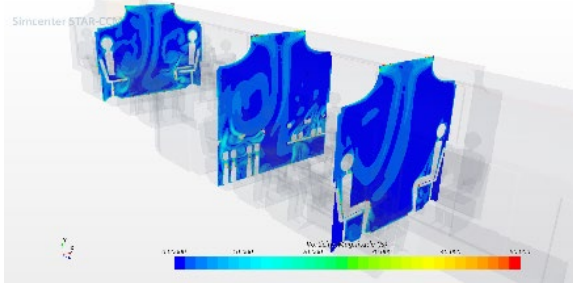
25 sec



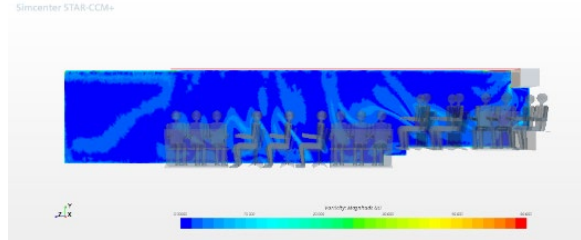
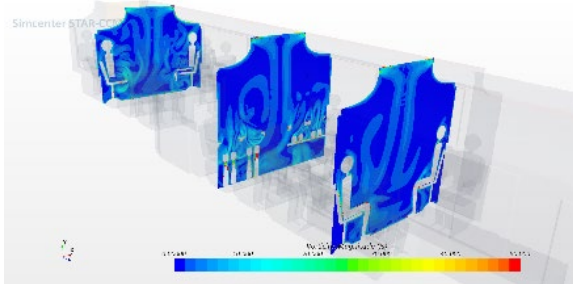
30 sec Doors closed



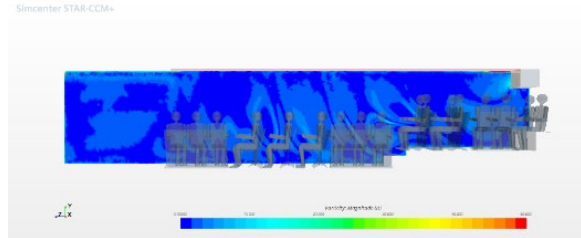
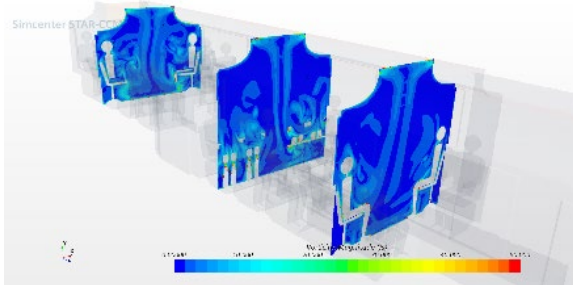
35 sec



40 sec



50 sec



60 sec

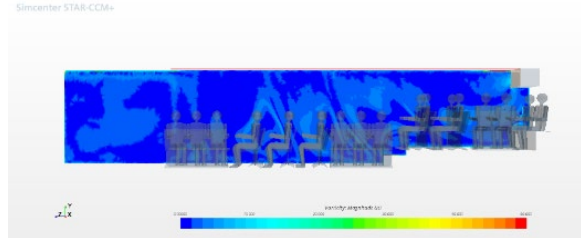
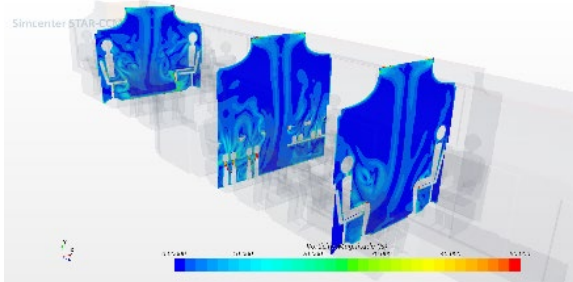
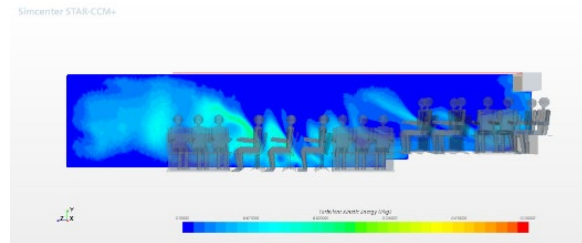
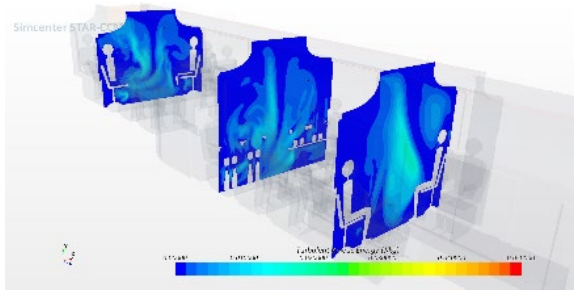
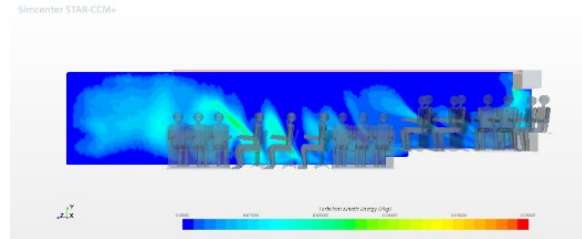
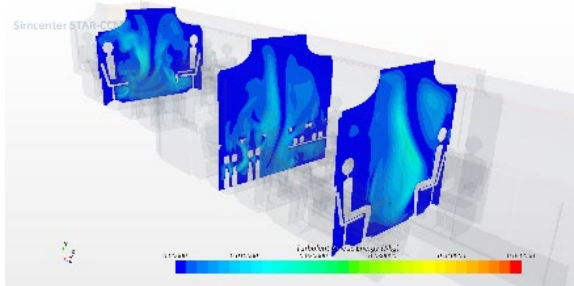


Figure 13. Contours of Turbulent Kinetic Energy (TKE) (2pp.)

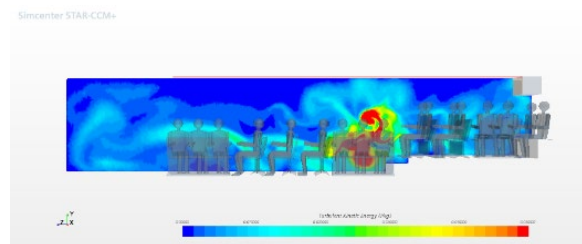
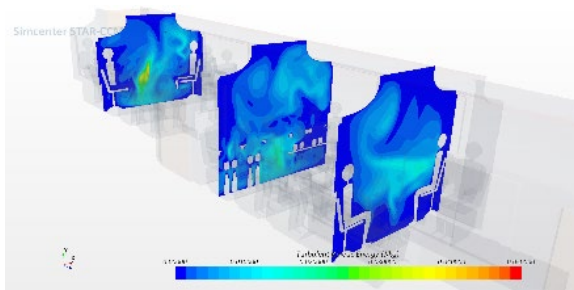
5 sec before doors opening



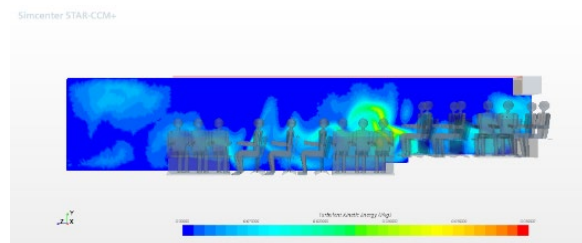
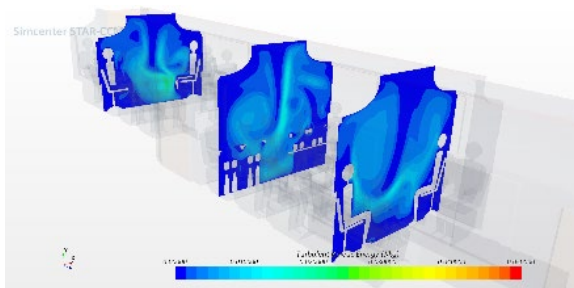
Doors opened



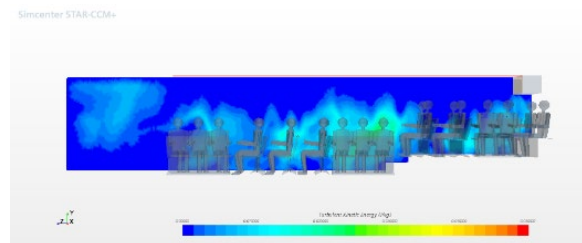
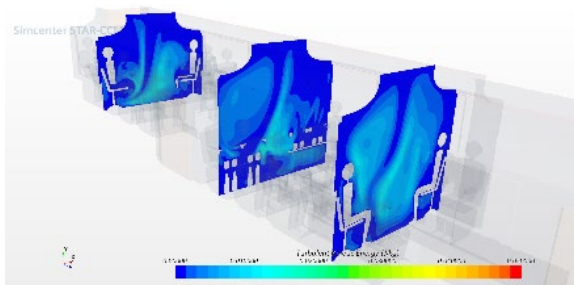
5 sec



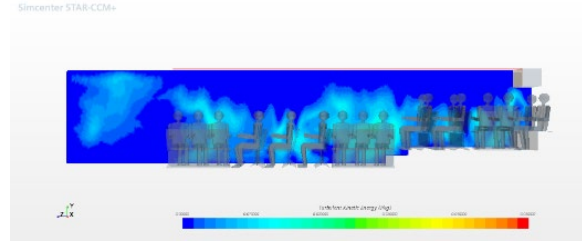
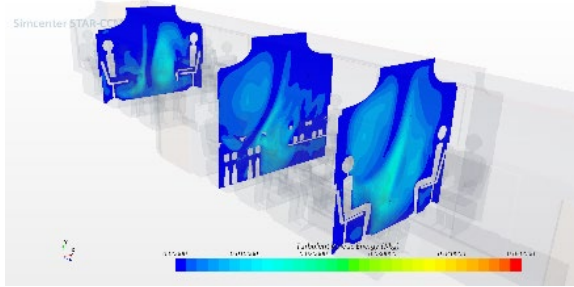
15 sec



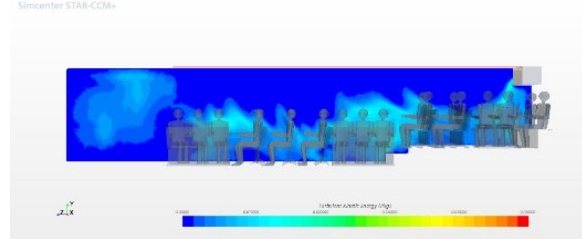
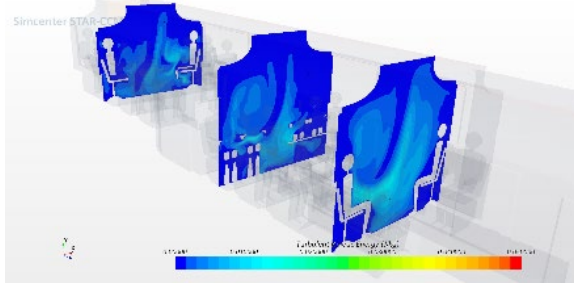
25 sec



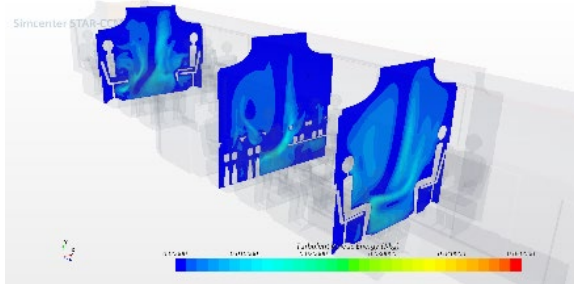
30 sec Doors closed



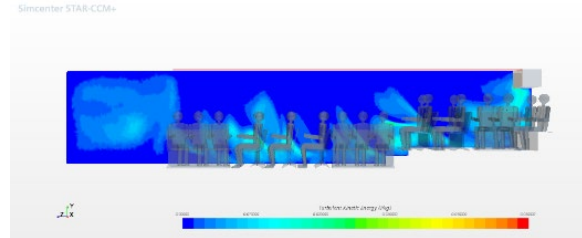
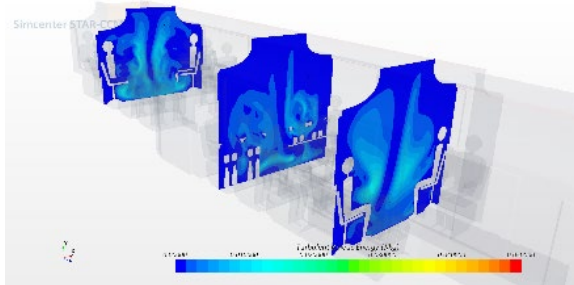
35 sec



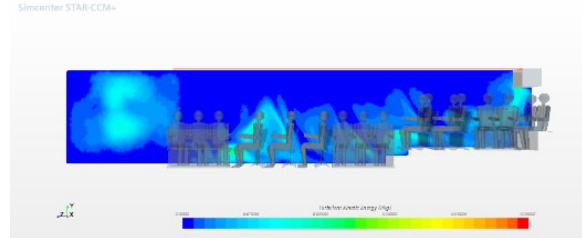
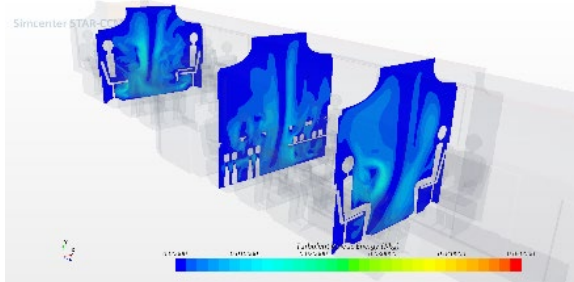
40 sec



50 sec



60 sec



IV. Conclusions

Unsteady three-dimensional incompressible Reynolds-Averaged Navier-Stokes (U-RANS) equations were solved, using the shear stress transport (SST) $k-\omega$ turbulence model, to investigate virus transport aboard a typical commuter bus with 37 sitting passengers. The study aimed at understanding virus distribution and infection rate for a passenger sitting in the middle of the bus and releasing 1,267 viruses/min; 2.5-micron particles were used to simulate aerosolized virus droplets. The computational fluid dynamics software Star CCM+ from Siemens on a Linux-based high-performance computing platform with 84 cores was used for all the simulations. Two cases were investigated: when the bus is in transit and when it is at a bus stop, unloading passengers. When the bus is in transit, results show high exposure for passengers sitting behind the infectious passenger. However, at the bus stop, due to air exchange, the viruses were transmitted to the seats in front of the infectious passenger, exposing passengers sitting in the front seats. The risk of infection is time-dependent, and with a high rate of ventilation, the number of infected passengers is estimated at 0.11 for 30 minutes of exposure.

Our recent investigation of virus transport aboard a commercial airplane¹⁵ at full capacity has shown that ventilation and wearing masks are significant factors in reducing infection aboard public transportation vehicles. In the present simulations, the ventilation rate per passenger was more than three times that inside a commercial airplane and thus the risk of infection was reduced significantly. With increased ventilation and air exchange outside, the virus's residence time is reduced, resulting in a reduced rate of infection.

Another significant result of the present investigation is the importance of having a well mixed air environment within the bus which should be of significance to the bus manufacturers. Our ongoing and future investigations include studying the impacts having multiple infectious passengers seated at different locations and longer traveling duration on the virus's transport and the rate of infection.

Endnotes

- ¹ S. Taherian, H.R. Rahai, J. Bonifacio, and R. Horstman, “Virus Transport Aboard Commercial Regional Jets,” The 44th AIAA Fluid Dynamics Conference, AIAA Aviation and Aeronautics Forum and Exposition, Atlanta, GA, June 2014.
- ² K.C. Klontz, “An Outbreak of Influenza a/Taiwan/1/86 H1N1 Infection at a Naval Base and Association with Airplane Travel,” *Am. J. Epidemiology* 129, no. 2 (1989): 341–348.
- ³ M. Moser, T.R. Bender, H.S. Margolis, G.R. Noble, A.P. Kendal, and D.G. Ritter, “An Outbreak of Influenza Aboard a Commercial Airline,” *Am. J. Epidemiology* 110, no. 1 (1979): 1–6.
- ⁴ W. Yang, S. Elankumaran, and L.C. Marr, “Concentration and Size Distributions of Airborne Influenza A Viruses Measured Indoors at a Health Center, Daycare Center, and Aeroplanes,” *J. R. Soc. Interface* (2018). doi:10.1098/rsif.2010.0686.
- ⁵ J. Yan, M. Grantham, J. Pantelic, J.B. de Masquita, B. Albert, F. Liu, S. Ehrman, D. Milton, and EMIT Consortium, “Infectious Virus in Exhaled Breath of Symptomatic Seasonal Influenza Cases from a College Community,” *PNAS* 115, no. 5 (2018): 1081–1086.
- ⁶ N. Nikitin, P. Ekaterina, E. Trifonova, and O. Karpova, “Influenza Virus Aerosols in the Air and Their Infectiousness,” *Adv. In Virology* (2014), Art IN 859090 2014, Hindawa Publishing.
- ⁷ R.H. Alfort, J.A. Kasel, P.J. Gerone, and V. Knight, “Human Influenza Resulting from Aerosol Inhalation,” *Proceeding of the Soc. Expe. Biology in Medicine* 122, no. 3 (1966): 800–804.
- ⁸ J. Fuhrman, G. Anderson, M.T. La Duc, Y. Piceno, G. Bearman, A. Dekas, D. Newcombe, K. Venkateswaran, T. Stuecker, and S. Osman, “A Comprehensive Assessment of Biologicals in Commercial Airline Cabin Air,” NASA, JPL, 2007.
- ⁹ M. Zuurbier, G. Hoek, P. van den Hazel, and B. Brunekreef, “Minute Ventilation of Cyclists, Car, and Bus Passengers: An Experimental Study,” *Environmental Health* 8, no. 48 (2009). doi:10.1186/1476-069x-8-48. PMC 2772854
- ¹⁰ S. Taherian, H.R. Rahai, and T. Waddington, “Particulates Depositions in Patient-Specific Simulations of Respiratory System,” Paper No. IMECE2014-36947, 2014 International Mechanical Engineering Congress & Exposition, November 2014, Montreal, Canada.
- ¹¹ S. Taherian, H.R. Rahai, B. Gomez, T. Waddington, and J. Bonifacio, “Tracheal Stenosis, A CFD Approach for Evaluation of Drug Delivery,” Paper No. IMECE2015-50799, ASME International Mechanical Engineering Conference & Exposition, Houston, TX, November 13–19, 2015.

¹² S. Taherian, H.R. Rahai, and D. Aguilar, “Effect of Nasal Cavity and Pharyngeal Regions on Airflow Simulation and Particle Depositions in Lower Generation of the Airways,” Paper No. IMEC2016-65305, ASME 2016 International Mechanical Engineering Congress & Exposition, November 11–17, 2016, Phoenix, AZ.

¹³ J. Bonifacio, H.R. Rahai, and S. Taherian, “The Effects of High-Frequency Oscillatory Flow on Particles’ Deposition in Upper Human Lung Airway,” Paper No. R16-8, 69th Annual Meeting of the American Physical Society Division of Fluid Dynamics, Portland, OR, November 20–22, 2016.

¹⁴ S. Taherian, H. Rahai, S. Lopez, J. Shin, and B. Jafari, “Evaluation of Human Obstructive Sleep Apnea Using Computational Fluid Dynamics,” *Communications Biology* (November 2019). <https://www.nature.com/articles/s42003-019-0668-z.pdf>

¹⁵ R. Horsman and H. Rahai, “A Risk of an Airborne Disease inside the Cabin of a Passenger Airplane,” SAE Technical Paper 2021-01-0036, 2021. doi:10.4271/2021-01-0036.

Bibliography

- Alfort, R.H., J.A. Kasel, P.J. Gerone, and V. Knight. "Human Influenza Resulting from Aerosol Inhalation." *Proceeding of the Soc. Expe. Biology in Medicine* 122, no. 3 (1966): 800–804.
- Bonifacio, J., H.R. Rahai, and S. Taherian. "The Effects of High-Frequency Oscillatory Flow on Particles' Deposition in Upper Human Lung Airway." Paper No. R16-8, 69th Annual Meeting of the American Physical Society Division of Fluid Dynamics, Portland, OR, November 20–22, 2016.
- Fuhrman, J., G. Anderson, M.T. La Duc, Y. Piceno, G. Bearman, A. Dekas, D. Newcombe, K. Venkateswaran, T. Stuecker, and S. Osman. "A Comprehensive Assessment of Biologicals in Commercial Airline Cabin Air." NASA, JPL, 2007.
- Horsman, R., and H. Rahai. "A Risk of an Airborne Disease inside the Cabin of a Passenger Airplane." SAE Technical Paper 2021-01-0036, 2021. doi:10.4271/2021-01-0036.
- Klontz, K.C. "An Outbreak of Influenza a/Taiwan/1/86 H1N1 Infection at a Naval Base and Association with Airplane Travel." *Am. J. Epidemiology* 129, no. 2 (1989): 341–348.
- Moser, M., T.R. Bender, H.S. Margolis, G.R. Noble, A.P. Kendal, and D.G. Ritter. "An Outbreak of Influenza Aboard a Commercial Airline." *Am. J. Epidemiology* 110, no. 1 (1979): 1–6.
- Nikitin, N., P. Ekaterina, E. Trifonova, and O. Karpova. "Influenza Virus Aerosols in the Air and Their Infectiousness." *Adv. In Virology* (2014), Art IN 859090 2014, Hindawa Publishing.
- Taherian, S., H. Rahai, S. Lopez, J. Shin, and B. Jafari. "Evaluation of Human Obstructive Sleep Apnea Using Computational Fluid Dynamics." *Communications Biology* (November 2019). <https://www.nature.com/articles/s42003-019-0668-z.pdf>.
- Taherian, S., H.R. Rahai, and D. Aguilar. "Effect of Nasal Cavity and Pharyngeal Regions on Airflow Simulation and Particle Depositions in Lower Generation of the Airways." Paper No. IMEC2016-65305, ASME 2016 International Mechanical Engineering Congress & Exposition, November 11–17, 2016, Phoenix, AZ.
- Taherian, S., H.R. Rahai, and T. Waddington. "Particulates Depositions in Patient-Specific Simulations of Respiratory System." Paper No. IMECE2014-36947, 2014 International Mechanical Engineering Congress & Exposition, November 2014, Montreal, Canada.
- Taherian, S., H.R. Rahai, B. Gomez, T. Waddington, and J. Bonifacio. "Tracheal Stenosis, A CFD Approach for Evaluation of Drug Delivery." Paper No. IMECE2015-50799, ASME International Mechanical Engineering Conference & Exposition, Houston, TX, November 13–19, 2015.

- Taherian, S., H.R. Rahai, J. Bonifacio, and R. Horstman. "Virus Transport Aboard Commercial Regional Jets." The 44th AIAA Fluid Dynamics Conference, AIAA Aviation and Aeronautics Forum and Exposition, Atlanta, GA, June 2014.
- Yan, J., M. Grantham, J. Pantelic, J.B. de Masquita, B. Albert, F. Liu, S. Ehrman, D. Milton, and EMIT Consortium. "Infectious Virus in Exhaled Breath of Symptomatic Seasonal Influenza Cases from a College Community." *PNAS* 115, no. 5 (2018): 1081–1086.
- Yang, W., S. Elankumaran, and L.C. Marr. "Concentration and Size Distributions of Airborne Influenza A Viruses Measured Indoors at a Health Center, Daycare Center, and Aeroplanes." *J. R. Soc. Interface* (2018). doi:10.1098/rsif.2010.0686.
- Zuurbier, M., G. Hoek, P. van den Hazel, and B. Brunekreef. "Minute Ventilation of Cyclists, Car, and Bus Passengers: An Experimental Study." *Environmental Health* 8, no. 48 (2009). doi:10.1186/1476-069x-8-48. PMC 2772854.

About the Authors

Hamid Rahai, PhD

Dr. Hamid Rahai is a professor in the Departments of Mechanical and Aerospace Engineering & Biomedical Engineering and the Associate Dean for Research and Graduate Studies in the College of Engineering at California State University, Long Beach (CSULB). He has taught various classes at the undergraduate and graduate levels in the areas of fluid dynamics, thermodynamics, heat transfer, instrumentation, numerical methods, and turbulence. He has supervised over 80 M.S. theses and projects and Ph.D. dissertations and has published more than 90 technical papers. He has received more than 10 million dollars in grants and contracts from the National Science Foundation, Federal Highway Administration, California Energy Commission, California Air Resources Board, Port of Los Angeles, Caltrans, Boeing Company, Southern California Edison, Long Beach Airport, and Long Beach Transit, among others. He has been granted a patent for the development of a high-efficiency vertical axis wind turbine (VAWT) and another with Via Verde Company on wind turbine apparatuses. He also has pending patents on a new conformal vortex generator tape for reducing wing-tip vortices, and one based on previous MTI-funded research for reducing NOx emissions of gas-powered engines using a humid air system. For the past 26 years, he has been a consultant to local energy and aerospace industries. Dr. Rahai is the recipient of several scholarly and creative activities awards (RSCA), including the 2012 CSULB Impact Accomplishment of the Year in RSCA Award, the 2002–2003 CSULB Distinguished Faculty RSCA Award, the 2004 Northrop Grumman Excellence in Teaching Award, and a 2005–06 Merit of Scholarship Award by the Southern California Chapter of the American Society of Heating, Refrigerating and Air Conditioning Engineers (ASHRAE). In 2014, Dr. Rahai received the Outstanding Engineering Educator Award from the Orange County Engineering Council in California, and in 2019 he was inducted as a senior member of the National Academy of Inventors (NAI).

Jeremy Bonifacio, PhD

Dr. Jeremy Bonifacio is a recent PhD graduate from the doctoral program in Engineering and Computational Mathematics, offered jointly between the CSULB College of Engineering and the Claremont Graduate University (CGU). He is a teaching professor and a research associate at the Center for Energy and Environmental Research & Services (CEERS) in the College of Engineering at California State University, Long Beach. He has been involved in various projects at CEERS related to emission control technologies and mitigations along with various aerodynamics and indoor air quality projects. He is the winner of the 2014 CSULB innovation challenge, co-owner of two provisional patents, and author of ten technical publications. Dr. Bonifacio's expertise is in experimental and computational fluid mechanics.

Hon. Norman Y. Mineta

MTI BOARD OF TRUSTEES

Founder, Honorable Norman Mineta*
Secretary (ret.),
US Department of Transportation

Chair, Abbas Mohaddes
President & COO
Econolite Group Inc.

Vice Chair, Will Kempton
Retired Transportation Executive

Executive Director, Karen Philbrick, PhD*
Mineta Transportation Institute
San José State University

Winsome Bowen
Chief Regional Transportation
Strategy
Facebook

David Castagnetti
Co-Founder
Mehlman Castagnetti
Rosen & Thomas

Maria Cino
Vice President
America & U.S. Government
Relations Hewlett-Packard Enterprise

Grace Crunican**
Owner
Crunican LLC

Donna DeMartino
Managing Director
Los Angeles-San Diego-San Luis
Obispo Rail Corridor Agency

John Flaherty
Senior Fellow
Silicon Valley American
Leadership Form

William Flynn *
President & CEO
Amtrak

Rose Guilbault
Board Member
Peninsula Corridor
Joint Powers Board

Ian Jefferies*
President & CEO
Association of American Railroads

Diane Woodend Jones
Principal & Chair of Board
Lea + Elliott, Inc.

David S. Kim*
Secretary
California State Transportation
Agency (CALSTA)

Therese McMillan
Executive Director
Metropolitan Transportation
Commission (MTC)

Jeff Morales
Managing Principal
InfraStrategies, LLC

Dan Moshavi, PhD*
Dean, Lucas College and
Graduate School of Business
San José State University

Toks Omishakin*
Director
California Department of
Transportation (Caltrans)

Takayoshi Oshima
Chairman & CEO
Allied Telesis, Inc.

Paul Skoutelas*
President & CEO
American Public Transportation
Association (APTA)

Beverley Swaim-Staley
President
Union Station Redevelopment
Corporation

Jim Tymon*
Executive Director
American Association of
State Highway and Transportation
Officials (AASHTO)

* = Ex-Officio

** = Past Chair, Board of Trustees

Directors

Karen Philbrick, PhD
Executive Director

Hilary Nixon, PhD
Deputy Executive Director

Asha Weinstein Agrawal, PhD
Education Director
National Transportation Finance
Center Director

Brian Michael Jenkins
National Transportation Security
Center Director

